Technical Note 1967-30

E. J. Kelly

Response of Seismic Arrays to Wide-Band Signals

29 June 1967

Prepared for the Advanced Research Projects Agency
under Electronic Systems Division Contract AF 19(628)-5167 by

Lincoln Laboratory
MASSACHUSETTS INSTITUTE OF TECHNOLOGY
Lexington, Massachusetts

MASSACHUSETTS INSTITUTE OF TECHNOLOGY

LINCOLN LABORATORY

RESPONSE OF SEISMIC ARRAYS TO WIDE-BAND SIGNALS

E. J. KELLY

Group 64

TECHNICAL NOTE 1967-30

29 JUNE 1967

LEXINGTON MASSACHUSETTS

ABSTRACT

Response patterns are computed for the LASA and other arrays and for a class of wide-band signals. Results are displayed as contour plots in wavenumber space and in real space, with and without P-wave attenuation.

Accepted for the Air Force
Franklin C. Hudson
Chief, Lincoln Laboratory Office

I. INTRODUCTION

It is usual to compute the response pattern of a seismic array for sinusoidal signals and to express the result as a function of relative wavenumber. These results are of limited usefulness because, on the one hand, real signals are wide-band transients and, on the other, it is difficult to interpret the wavenumber-space pattern in terms of array performance in real space.

In this report a simple theory is developed for the response of an array to wide-band signals, and patterns are computed using a signal model characterized by a Gaussian power spectrum. The results are shown as contour plots, both in wavenumber space and in real space. The real space patterns are computed for an event at a fixed epicenter and the response is given as a function of the point to which the array is steered. This pattern, of course, depends upon the reference epicenter. Analogous patterns are computed for the case of an array steered at a fixed reference point, the response being shown as a function of source epicenter. These patterns differ from the former ones by the addition of the effect of attenuation on the P-wave signal.

II. ARRAY BEAM RESPONSE TO WIDE-BAND SIGNALS

We suppose that we have an array of N identical sensors (such as short-period vertical-component seismometers) located at the points $\underline{r}_n$ in a plane at or near the earth's surface. The origin of coordinates serves as a reference point within the array. Let a transient signal propagate across the array towards a direction bearing β (to the East of North) with a horizontal phase velocity v. We assume that the waveform at the origin is

$$s(t) = \int_{-\infty}^{\infty} S(\omega)\, e^{i\omega t}\, d\omega/2\pi$$

and that the propagation is locally non-dispersive, so that the signal observed at the n^{th} sensor is simply

$$x_n(t) = s(t - \underline{\alpha} \cdot \underline{r}_n) \ .$$

In this formula we have introduced the slowness vector, $\underline{\alpha}$, which points in the direction of propagation and has magnitude $|\underline{\alpha}| = 1/v$, in seconds per kilometer. The slowness is determined directly from the travel-time curve, $T(\Delta)$, (travel-time as a function of linear distance to source) by means of the relation

$$|\underline{\alpha}| = \frac{dT}{d\Delta} \ .$$

In order to focus the array on a signal characterized by slowness vector $\underline{\alpha}$ we form a beam by introducing steering delays and adding the sensor outputs. The resulting beam output is

$$b(t) \equiv \frac{1}{N} \sum_{n=1}^{N} x_n(t + \underline{\alpha} \cdot \underline{r}_n) \ .$$

Much more complicated forms of array processing have been used,[1] but we are interested here only in the simple beamforming technique just described. It can be shown that simple beamforming is an optimum procedure to use in the case of broadband background noise which is uncorrelated between sensors.

Now suppose that we steer a beam for slowness vector $\underline{\alpha}$ and a signal arrives with slowness vector $\underline{\alpha}'$. Combining the definitions given above, we see that the resulting beam output is

$$b(t) = \int_{-\infty}^{\infty} S(\omega) \left\{ \frac{1}{N} \sum_{n=1}^{N} \exp\left[i\omega(\underline{\alpha} - \underline{\alpha}') \cdot \underline{r}_n \right] \right\} e^{i\omega t} \, d\omega/2\pi \ .$$

That component of the signal having angular frequency ω is propagating with angular wavenumber vector $\omega\underline{\alpha}'$, and at that frequency the array is steered for wavenumber vector $\omega\underline{\alpha}$. The result is that this frequency component of the signal is multiplied by the factor $F(\omega\underline{\alpha}' - \omega\underline{\alpha})$, where

$$F(\underline{k}) \equiv \frac{1}{N} \sum_{n=1}^{N} \exp\left[-i\underline{k} \cdot \underline{r}_n \right]$$

is the wavenumber response function of the array. Note that the beam output depends only on the difference vector, $\underline{\beta} = \underline{\alpha}' - \underline{\alpha}$, between the two slowness vectors.

The pattern of the array in wavenumber space, defined as

$$P(\underline{k}) = |F(\underline{k})|^2 ,$$

actually shows the array response to narrow-band signals. Since wide-band signals suffer distortion of waveform in passing through the beamforming operation, the wide-band array response cannot be fully characterized by a single numerical pattern. However, there are various ways of assigning a single number to the beam response to a given signal which serve to characterize the effective pattern in an approximate way. Of these, the most tractable, mathematically, is the total energy received on the beam, ..e.,

$$\int_{-\infty}^{\infty} b(t)^2 \, dt ,$$

for a signal which is itself of finite total energy. In practice, it is usual to form a family of beams, using a grid of steering points, and measure the signal slowness vector (which in turn determines the event's epicenter) by making some kind of decision as to which beam is "best," or by interpolating between beams. If this is to be done automatically, it must be based on some functional of the beam output, such as

the beam energy, average absolute value, peak value, etc. Some justification for using the energy as an optimum functional can be made from statistical considerations, and this functional will be used throughout this report.

We substitute the wavenumber response function, $F(\underline{k})$, into the formula for b(t), with the result

$$b(t) = \int_{-\infty}^{\infty} S(\omega)\, F[\omega(\underline{\alpha}' - \underline{\alpha})]\, e^{i\omega t}\, d\omega/2\pi \,.$$

Now, using Parseval's theorem, we can evaluate the effective pattern of the beam:

$$E(\underline{\beta}) \equiv \int_{-\infty}^{\infty} b(t)^2\, dt = \int_{-\infty}^{\infty} |S(\omega)|^2\, |F(\omega \underline{\beta})|^2\, d\omega/2\pi$$

$$= \int_{-\infty}^{\infty} |S(\omega)|^2\, P(\omega \underline{\beta})\, d\omega/2\pi \,,$$

where $\underline{\beta} = \underline{\alpha}' - \underline{\alpha}$ is the slowness difference vector which describes the relative position of the beam and the signal. We assume that the signal power spectrum is normalized so that

$$\int_{-\infty}^{\infty} |S(\omega)|^2\, d\omega/2\pi = 1 \,,$$

since in this case $E(0) = 1$ and $E(\beta)$ then measures the relative response to events not in the beam center.

Suppose we represent the signal power spectrum in the form

$$|S(\omega)|^2 = \frac{1}{2}\{G(\omega - \omega_o) + G(-\omega - \omega_o)\}$$

where $G(\omega)$ is a normalized function,

$$\int_{-\infty}^{\infty} G(\omega)\, d\omega/2\pi = 1 ,$$

which is more or less peaked at $\omega = 0$. The idea is to recognize explicitly a "center frequency," ω_o, for the signal, even though the bandwidth may be relatively large. The two terms are required to insure the necessary symmetry of $|S(\omega)|^2$. Since $P(\omega \underline{\beta})$ is symmetric in ω, we have

$$E(\underline{\beta}) = \int_{-\infty}^{\infty} G(\omega - \omega_o)\, P(\omega \underline{\beta})\, d\omega/2\pi$$

$$= \int_{-\infty}^{\infty} G(\omega)\, P[(\omega + \omega_o)\underline{\beta}]\, d\omega/2\pi$$

$$= N^{-2} \sum_{n,m=1}^{N} \int_{-\infty}^{\infty} G(\omega) \exp[i(\omega + \omega_o)\underline{\beta}\cdot(\underline{r}_n - \underline{r}_m)]\, d\omega/2\pi$$

$$= N^{-2} \sum_{n,m=1}^{N} \exp[i\omega_o \underline{\beta}\cdot(\underline{r}_n - \underline{r}_m)] \int_{-\infty}^{\infty} G(\omega) \exp[i\omega \underline{\beta}\cdot(\underline{r}_n - \underline{r}_m)]\, d\omega/2\pi .$$

The single-frequency case (at $\omega = \omega_o$) can be recovered by replacing $G(\omega)$ by a delta function at the origin with the expected result

$$E(\underline{\beta}) = \left|\frac{1}{N}\sum_{n=1}^{N} \exp\left[i\omega_o \underline{\beta}\cdot\underline{r}_n\right]\right|^2 = P(\omega_o \underline{\beta}) .$$

In general, if we put

$$g_{n,m} \equiv \int_{-\infty}^{\infty} G(\omega) \exp\left[i\omega \underline{\beta}\cdot(\underline{r}_n - \underline{r}_m)\right] \, d\omega/2\pi ,$$

then

$$E(\underline{\beta}) = N^{-2} \sum_{n,m=1}^{N} g_{n,m} \exp\left[i\omega_o \underline{\beta}\cdot(\underline{r}_n - \underline{r}_m)\right] .$$

Since the matrix, $g_{n,m}$, is real and symmetric and has diagonal values of unity, we obtain

$$E(\underline{\beta}) = \frac{1}{N} + \frac{2}{N^2} \sum_{n>m=1}^{N} g_{n,m} \cos\left[\omega_o \underline{\beta}\cdot(\underline{r}_n - \underline{r}_m)\right] .$$

In order to get an idea of the effect of the wide-band nature of the signals, we shall make a simple assumption for the spectral function, $G(\omega)$, namely a Gauss function:

$$G(\omega) = (2\pi\sigma^2)^{-1/2} \exp\left\{-\frac{1}{2\sigma^2}\left(\frac{\omega}{2\pi}\right)^2\right\} .$$

Plots of the resulting signal power spectra are shown in Fig. 1 for a center frequency of 1 Hz and a series of values of σ (effective bandwidth). The frequencies f_+ and f_- shown on each graph are the 3-db points.

For this spectrum we find the matrix

$$g_{n,m} = \exp\{-\frac{1}{2}(\sigma/f_o)^2 [\omega_o \underline{\beta} \cdot (\underline{r}_n - \underline{r}_m)]^2\}$$

where $f_o \equiv \omega_o/2\pi$ is the center frequency in Hertz. Note that $\omega_o \underline{\beta} \equiv \underline{k}_o$ is the wave-number difference vector corresponding to the center frequency. Again, the single-frequency case is recovered simply by putting $\sigma = 0$. It should also be noted that the wide-band pattern is formally equivalent to a single-frequency pattern, computed as a sum over points $(\underline{r}_n - \underline{r}_m)$ in lag space, with a taper, or set of weights (in our special case these are Gaussian) applied in lag space. Using this analogy we may expect the result of the finite signal bandwidth, in general, to be a broadening of the main lobe and an evening out of the response elsewhere; including a reduction of sidelobes. Also, grating lobes (i.e., sidelobes as large as the main lobe) due to regularities in array geometry, if present, will be reduced to the status of sidelobes.

It can also be seen directly from our first formula for $E(\underline{\beta})$ that it is essentially an average of values of $P(\underline{k})$ over a range of $\underline{k}$-values in the direction of $\underline{\beta}$. The larger the magnitude of $\underline{\beta}$, the larger the interval of averaging, hence the pattern-smearing becomes progressively more pronounced with distance from the origin in the $\underline{\beta}$-plane. These phenomena can be clearly seen in the contour plots of Section III.

III. ARRAY RESPONSE PATTERNS IN WAVENUMBER SPACE AND IN REAL SPACE

Using the Gaussian signal model and the pattern definition of Section II, computations have been made for a number of array geometries. In the first series of contour diagrams, the patterns are shown (in terms of db down from the value at the origin), plotted in wavenumber space. The wavenumber difference vector corresponding to the vector $\underline{\beta}$ is defined as

$$\Delta\underline{\not k}_o \equiv f_o \underline{\beta} ,$$

where we have used the Δ to symbolize the fact that the argument of the pattern function is a difference vector, and the slash identifies the cyclic wavenumber, in cycles per kilometer, corresponding to the use of f_o instead of ω_o. In terms of $\Delta\underline{\not k}_o$, the formula on which the computations are based is

$$E(\Delta\underline{\not k}_o) = \frac{1}{N} + \frac{2}{N^2} \sum_{n>m=1}^{N} \exp\left\{-\frac{1}{2} b_f^2 [2\pi\Delta\underline{\not k}_o \cdot (\underline{r}_n - \underline{r}_m)]^2\right\} \cos[2\pi\Delta\underline{\not k}_o \cdot (\underline{r}_n - \underline{r}_m)] .$$

Here, $b_f \equiv \sigma/f_o$ is a measure of fractional bandwidth. Note that this function is symmetric with respect to the sign of the vector, $\Delta\underline{\not k}_o$.

In Fig. 2 we show a scaled map of the LASA array, treating each of the 21 subarrays as single sensors. The main lobe of the response pattern of this array in wavenumber space is shown in Fig. 3 for a single frequency signal at 1 Hz, and in

Figures 4 through 8 for a series of values of bandwidth,* namely σ = 0.1, 0.2, 0.3, 0.4 and 0.5 Hz. The broadening of the main lobe is clearly shown, as well as the filling-in of the low-points in the pattern in the upper-right and lower-left hand corners. For comparison with later figures, the LASA response for the case $(\sigma/f_0) = 0.2$ is shown in Fig. 23 for a larger range of values of wavenumber.

A similar series of figures for a typical LASA subarray (F2) is shown in Figs. 9 through 15. The very regular geometry of this array (Fig. 9) gives rise to a complex pattern for a sinusoidal signal (Fig. 10), featuring deep nulls. These features are progressively smoothed by increasing bandwidth until we reach the case of Fig. 15, which gives no hint of the complexity of the single-frequency case.

A final series of plots shows the effect of bandwidth on grating lobes. Figure 16 shows a simple four-element array. Its single-frequency response over a relatively large portion of wavenumber space is shown in Fig. 17, where many grating lobes (zero db response) are shown. The sequence of Figs. 18 through 22 corresponding to the same five values of bandwidth as before ends with a pattern showing a main lobe against a background level nearly flat at 6 db down from the origin.

It is, of course, much more convenient to study the array pattern directly in real space, i.e., in latitude and longitude, instead of in wavenumber space. The

---

* In these figures the σ-values are labelled in Hertz, which is correct for a center frequency of 1 Hz. However, the patterns apply to any center frequency and a fractional bandwidth, b_f, numerically equal to the indicated σ (in other words the pattern labelled "σ = 0.2 Hz" applies to any center frequency, f_0, and a Gaussian spectrum with variance parameter $\sigma = 0.2\ f_0$).

disadvantage, however, is that the pattern varies with the point to which the array is steered. The procedure is to pick a steering point, say latitude φ_o, longitude λ_o, and then compute the wavenumber vector $\underline{k}_o(\varphi_o, \lambda_o)$ which corresponds to this point, as seen from the array. This vector points away from the steering point, i.e., it points in the direction $\pi + \beta$, where β is the bearing of (φ_o, λ_o) as seen from the array center, and has magnitude

$$|\underline{k}_o(\varphi_o, \lambda_o)| = \omega_o \alpha_o,$$

where α_o is the slowness and ω_o is the signal center frequency in radians. The pattern at any arbitrary point (φ, λ) is then computed by first finding the relevant wavenumber vector, $\underline{k}(\varphi, \lambda)$, then putting

$$\Delta\underline{k}_o = (1/2\pi)(\underline{k}_o - \underline{k}),$$

and using the formulas given at the beginning of this Section. Since the pattern is symmetrical with respect to the sign of $\Delta\underline{k}_o$, it doesn't matter whether we compute our wavenumber vectors pointing away from or towards the aiming point, so long as we are consistent. It is also true that the array response is unchanged by interchanging the points to which the array is steered and the location of the hypothetical event, so long as signal attenuation is ignored, since this interchange only results in a change in the sign of $\Delta\underline{k}_o$.

For a study of the ability of an array to locate events by forming a number of beams at various steering points, we may think of the event as fixed at a reference point, (φ_o, λ_o), while the beam is steered to a variable point, (φ, λ). The response at (φ, λ), relative to the response at the actual event location, then determines the pattern of interest. This pattern is simply the wavenumber pattern transformed to a new coordinate system.

However, it also makes sense to steer a beam at a fixed point, (φ_o, λ_o), and consider the array response to an event of fixed magnitude occurring at a variable point, (φ, λ). Normalized to the response when (φ, λ) coincides with (φ_o, λ_o), this pattern differs from the former in that the signal attenuation (computed from empirical Q-factors) for a source at (φ, λ), relative to the attenuation at (φ_o, λ_o) must be taken into account. The resulting pattern describes the response to an unwanted event (or body-wave noise) with a source (or apparent source) at some point other than that of a possible event to which the array is steered. In the first pattern (the "beamforming pattern") the response is nowhere higher than at the reference point, (φ_o, λ_o). In the second pattern the response will often be greater off-center than at the reference, since locations usually exist with sufficiently less attenuation than at beam center to more than offset the rejection due to being off the center of the array main beam.

These features are illustrated in a series of figures, starting with Fig. 26. In these figures the reference point is at the center, indicated by a star, and the contours are labelled in db down from this reference point. In Fig. 26 we show the LASA

beamforming pattern for a hypothetical event on the coast of Peru, 70° from the array. For this and all subsequent patterns the signal was assumed to have a center frequency of 1 Hz and a "fractional bandwidth," $b_f = \sigma/f_o$, of 0.2. The signal power spectrum is 3 db down from its peak value at the frequencies 0.76 Hz and 1.24 Hz for this case, which seems fairly realistic. The distortion of the wavenumber space pattern (see Fig. 23) when transformed to real space is rather severe. In Fig. 27 the corresponding pattern is shown with attenuation added. The curve of Q-factor versus distance which was used is shown in Fig. 25. The shaded area in Fig. 27 is a region of response greater than or equal to the response at the reference point. This results from the fact that the Q-factor curve dips, just beyond 70°, resulting in less attenuation with greater distance for a few degrees. The result is to shift the maximum of the pattern. The effect of large attenuation in and beyond the core shadow boundary (lower right-hand corner) is also clearly seen.

A more dramatic case is shown in Figs. 28 and 29, where the reference point is at 48° from the LASA array (a point in Colombia was chosen), which is at a local peak between two dips in the Q-factor curve. The beamforming pattern is again a distorted version of the wavenumber pattern, but now the pattern including the Q-factor (Fig. 29) is strongly modified by the various peaks and troughs of the Q-factor curve.

A final pair of patterns, Figs. 30 and 31, using a reference point in Japan, 90° from the LASA array, was computed for an array comprising of D, E, and F rings only from the LASA array (12 elements). The corresponding wavenumber pattern is

given in Fig. 24. The main lobe is considerably smaller than for the full array, and the troublesome 6 db sidelobes which can be seen in Fig. 23 are absent.

REFERENCE

1. J. Capon, R. J. Greenfield, R. T. Lacoss and R. J. Kolker, "Short-Period Signal Processing Results for the Large Aperture Seismic Array," M.I.T., Lincoln Laboratory JA-3071, submitted to Geophysics, 1967.

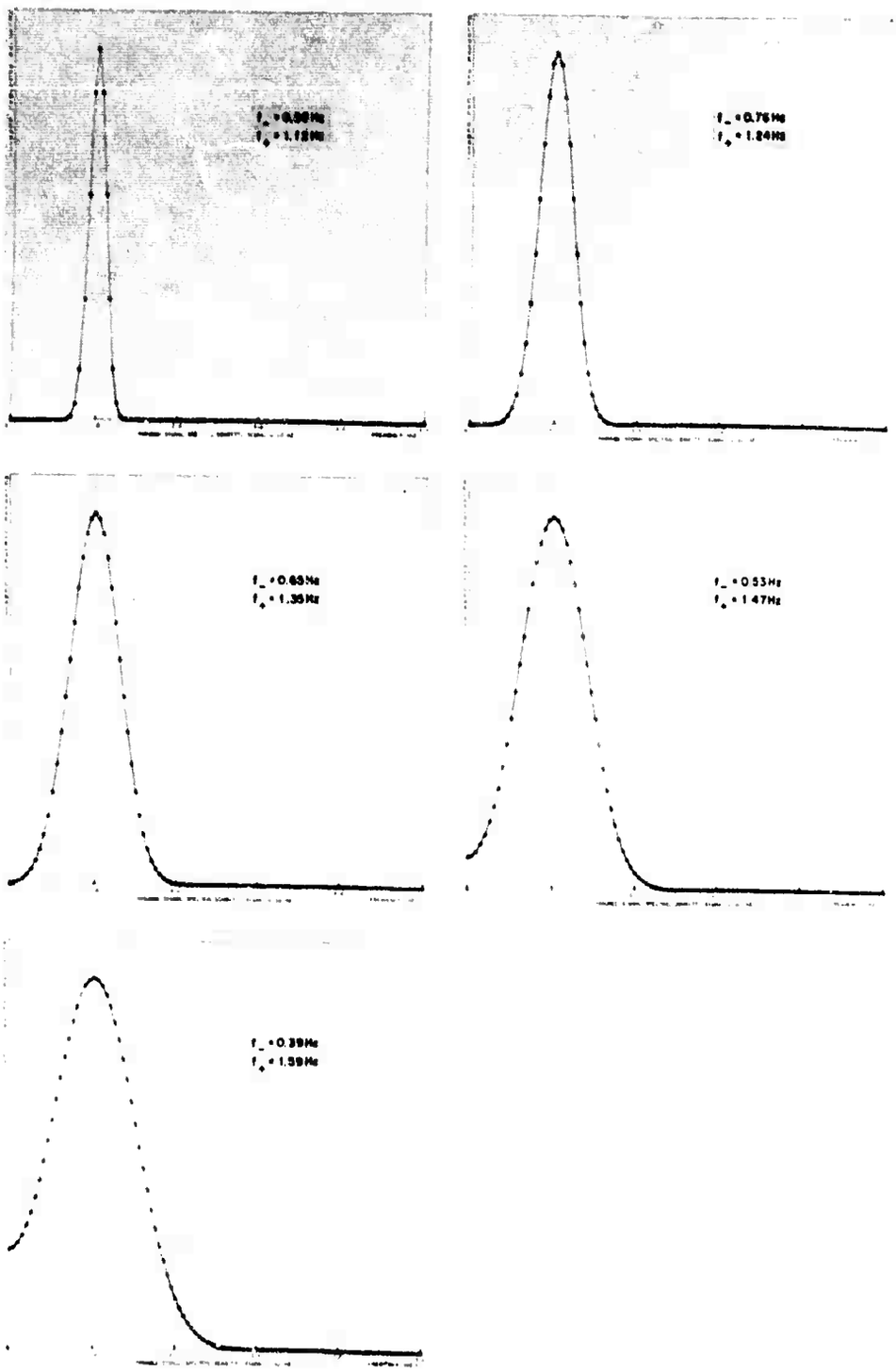

Figure 1 Signal spectra for a center frequency of 1.0 Hz and various values of σ. Three db frequencies labelled as $f_{\pm}$.

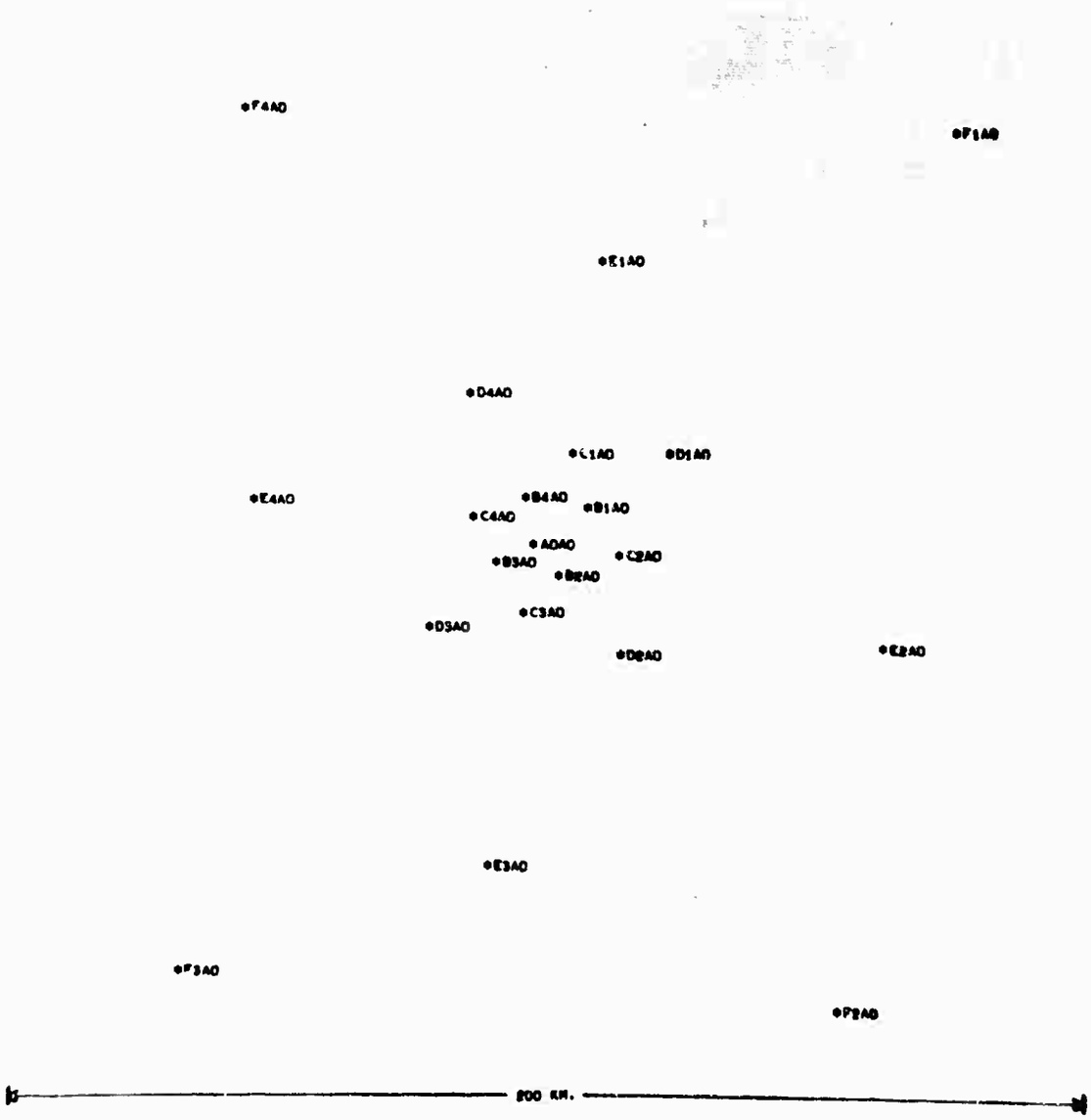

Figure 2 The LASA array (symbols are site names).

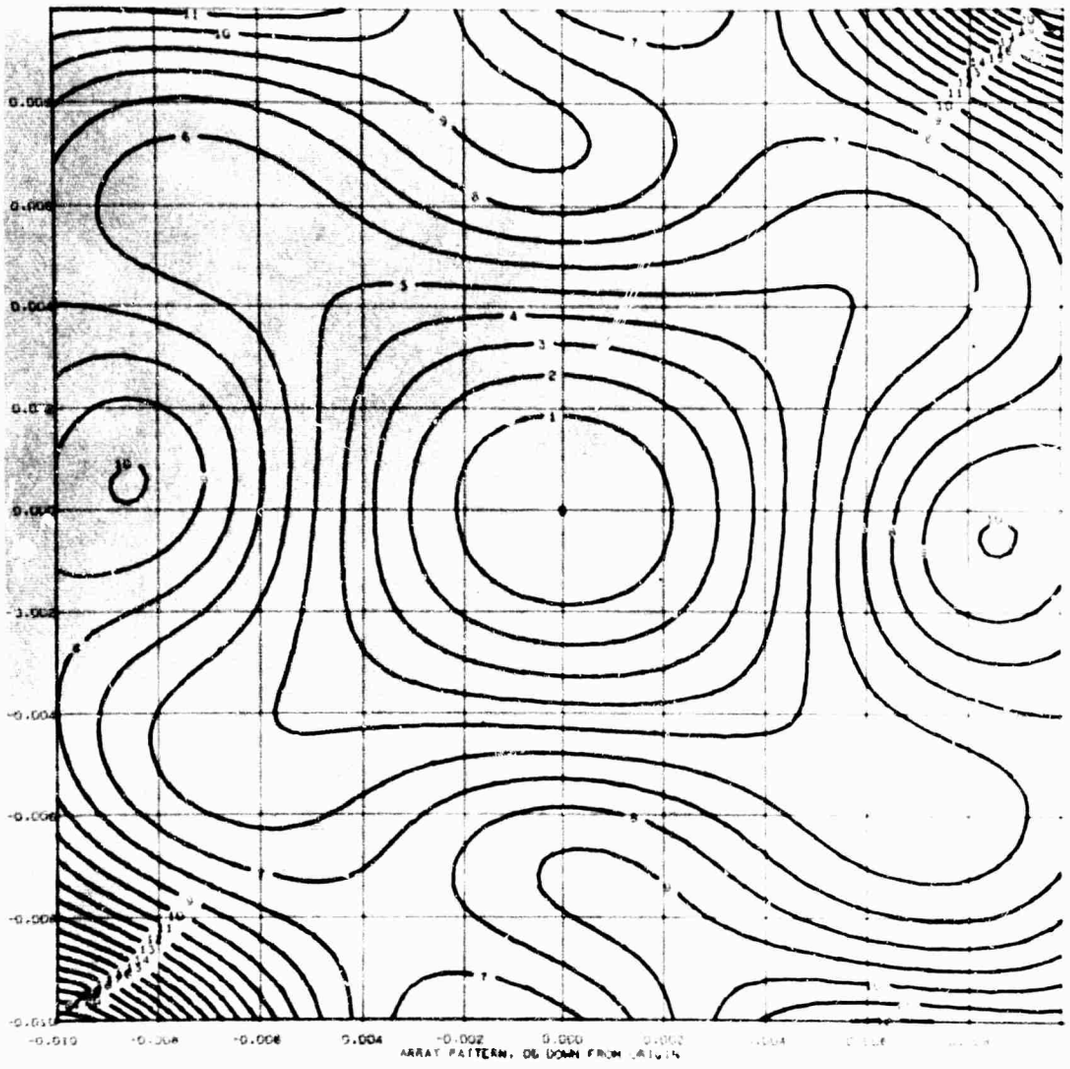

Figure 3 LASA main beam. $\sigma = 0.0$

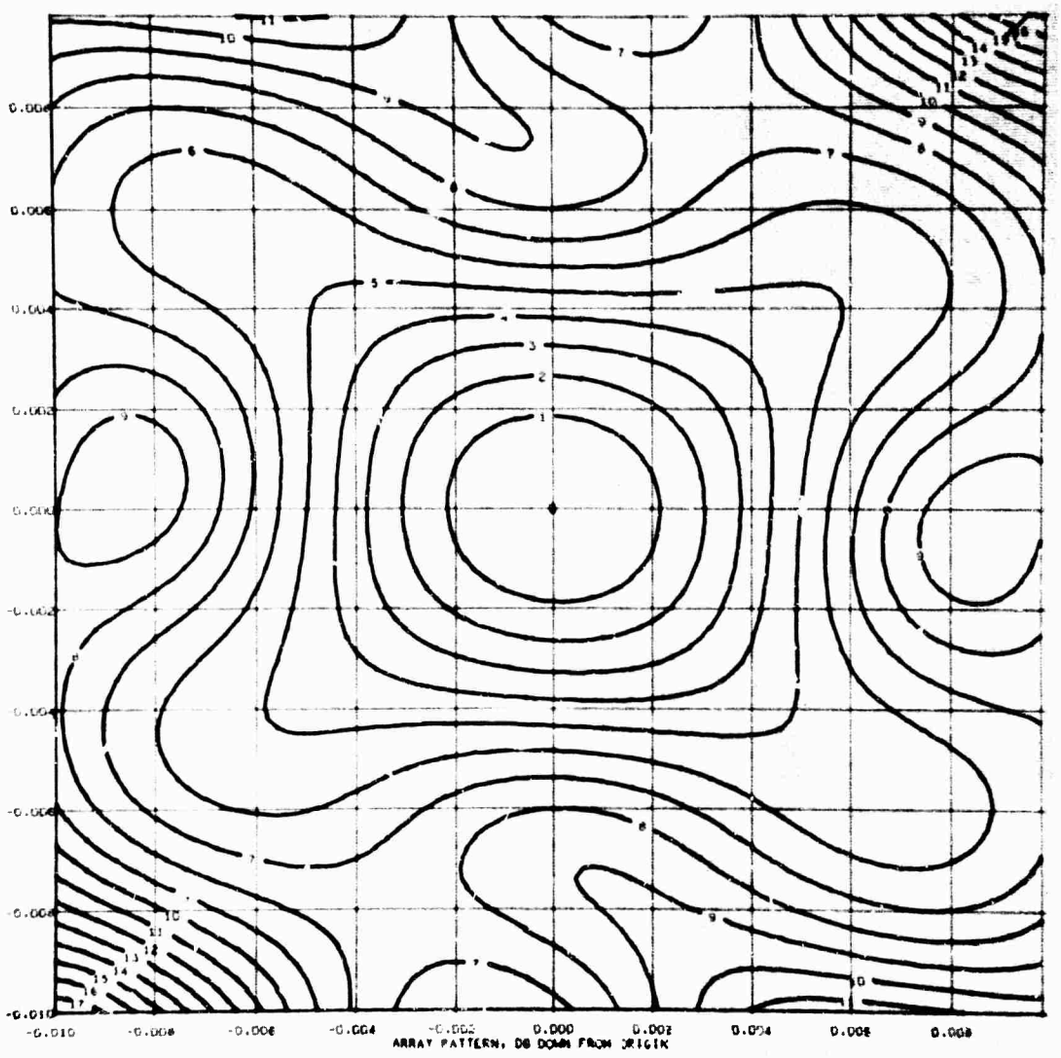

Figure 4 LASA main beam. $\sigma = 0.1$

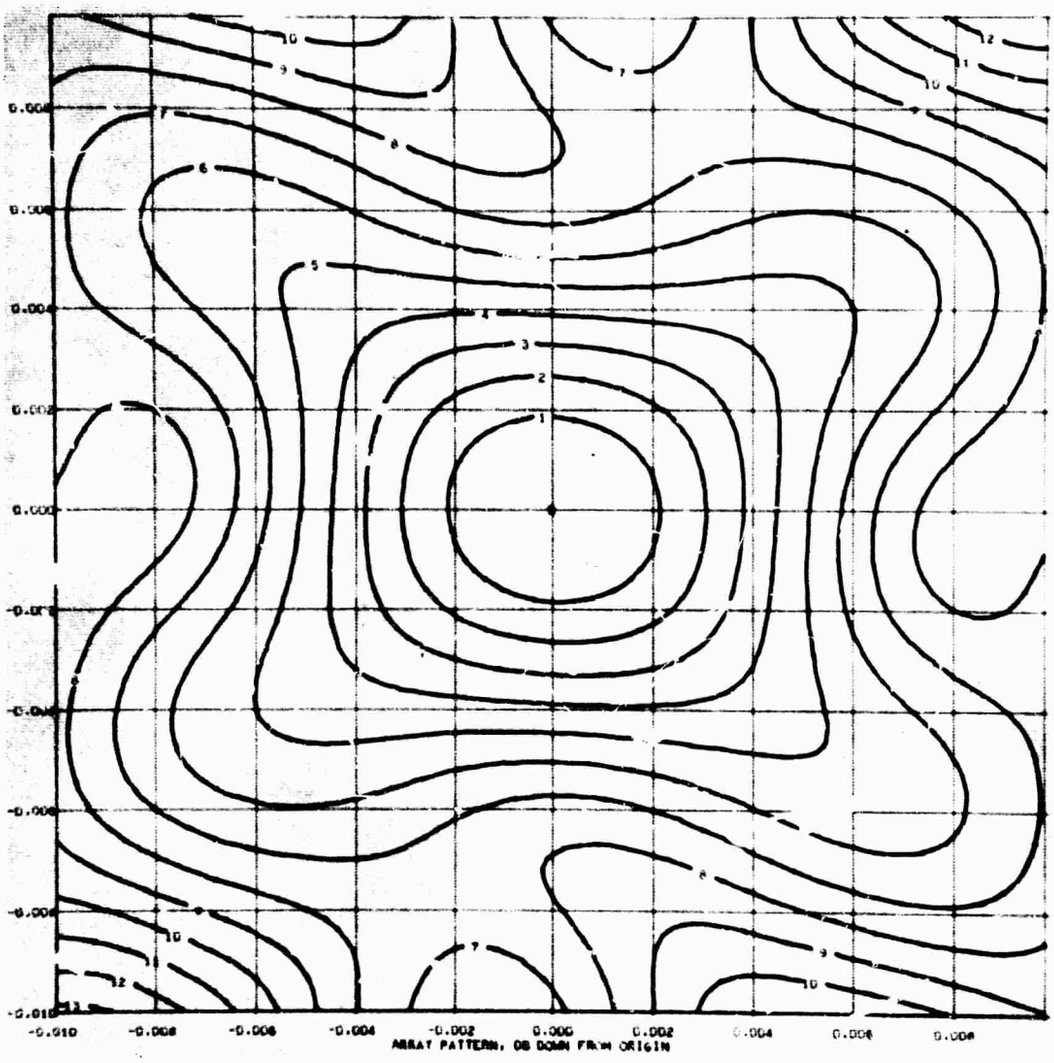

Figure 5 LASA main beam. $\sigma = 0.2$

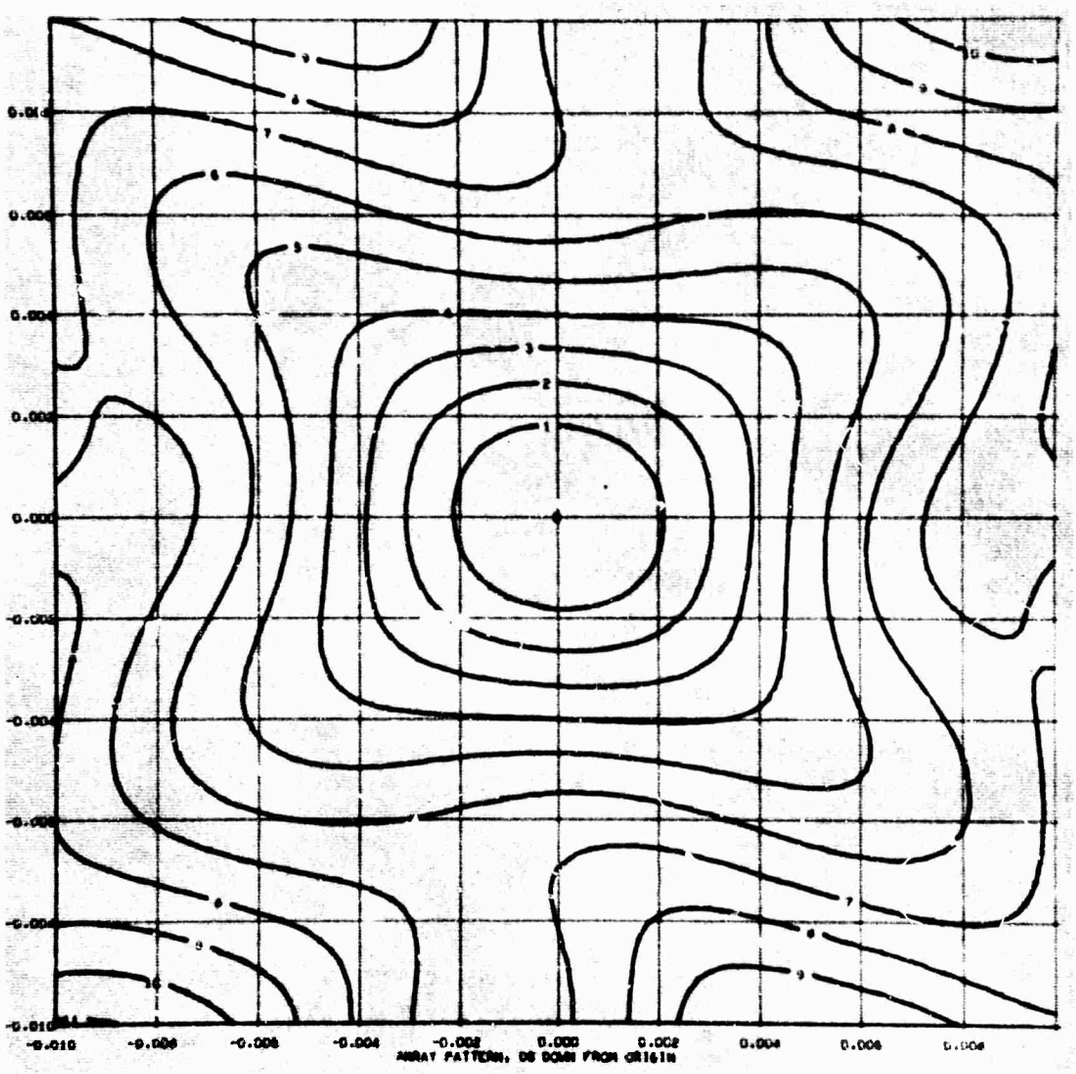

Figure 6 LASA main beam. $\sigma = 0.3$

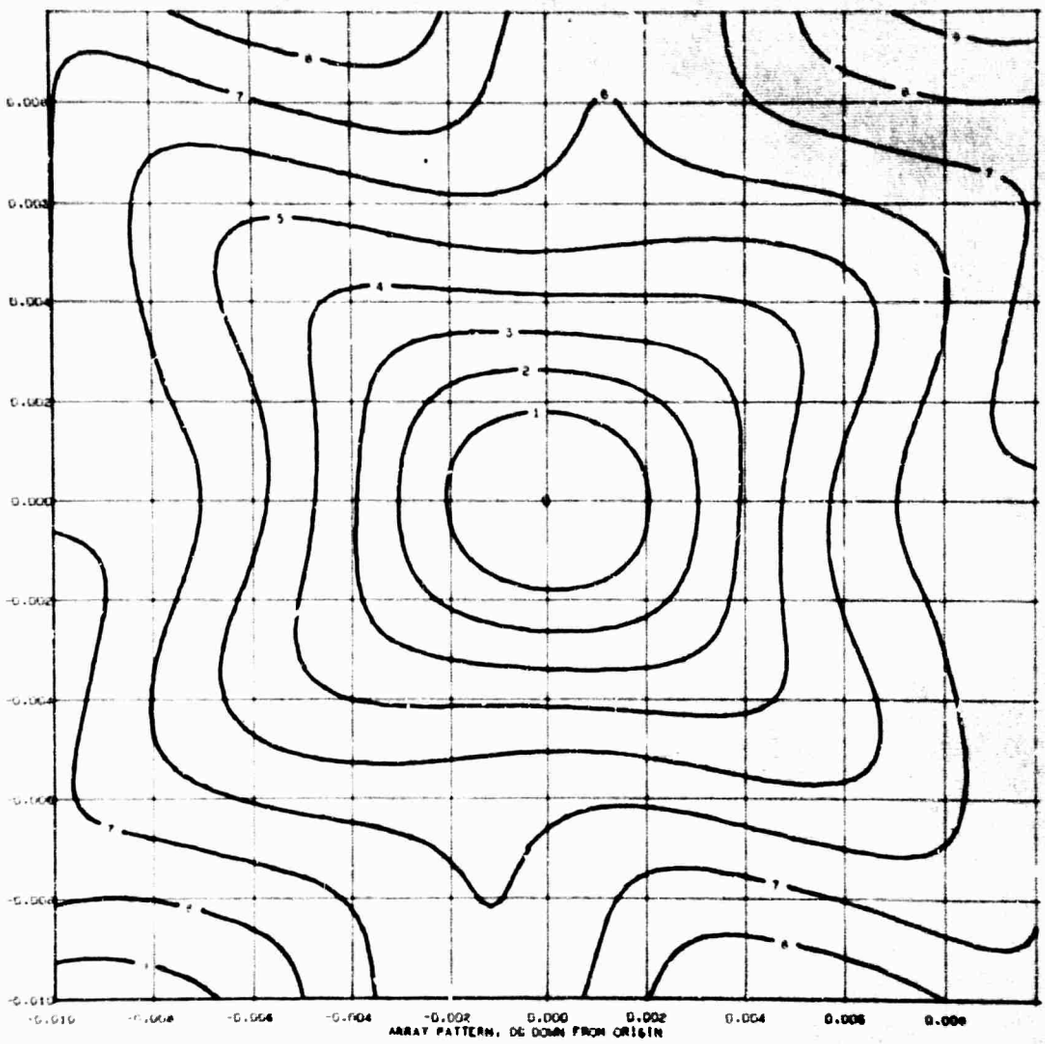

Figure 7 LASA main beam. $\sigma = 0.4$

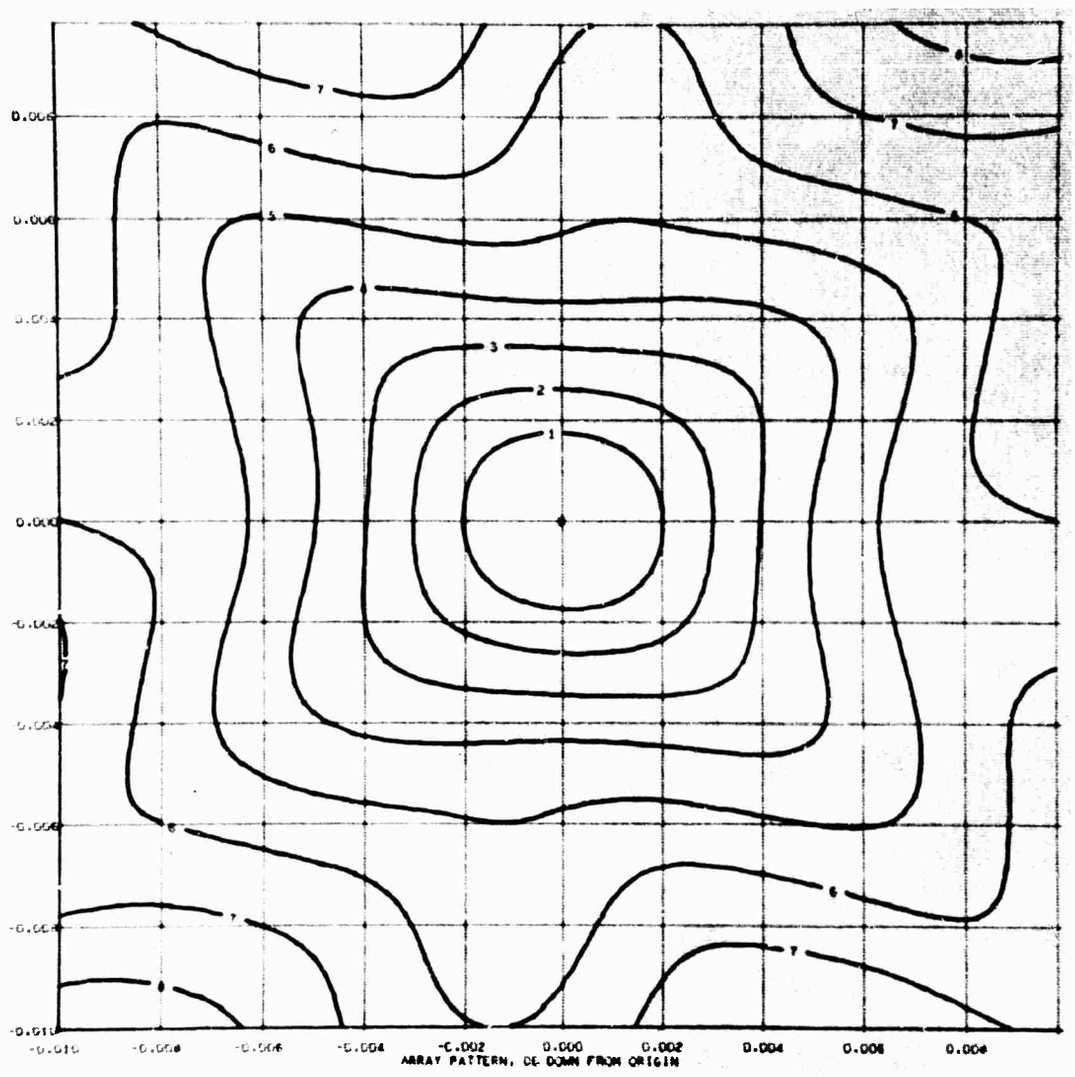

Figure 8 LASA main beam. $\sigma = 0.5$

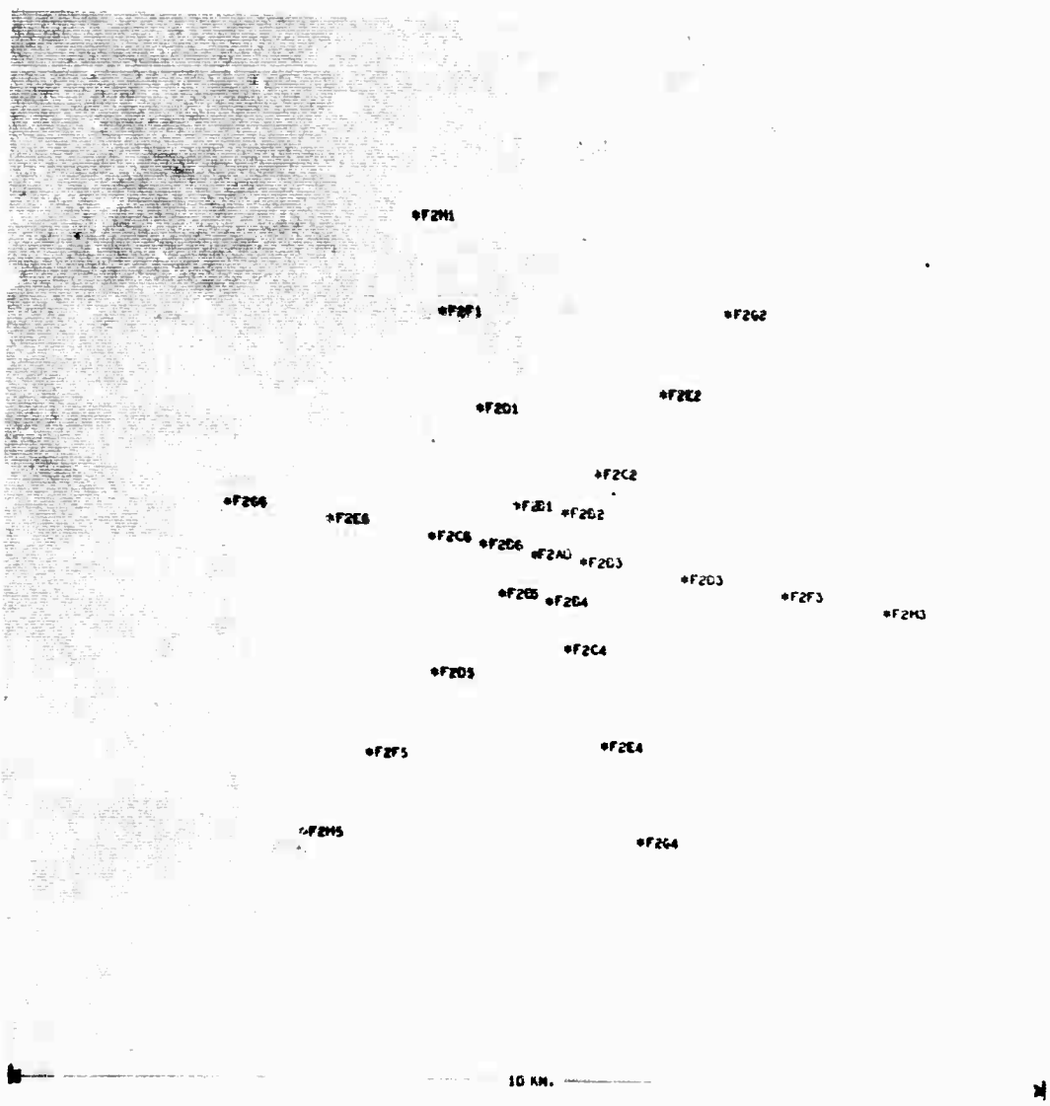

Figure 9 Subarray F2 of the LASA array.

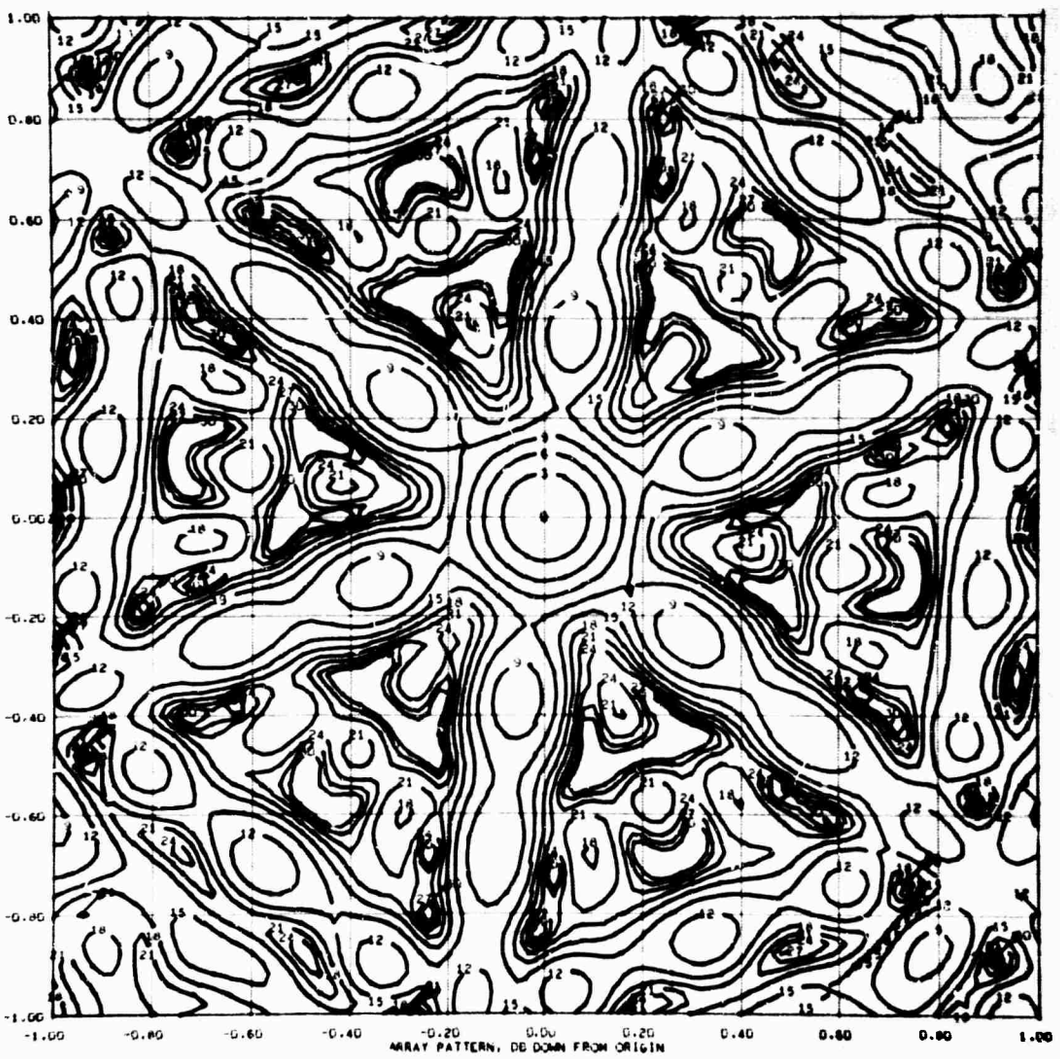

Figure 10 Subarray pattern. $\sigma = 0.0$

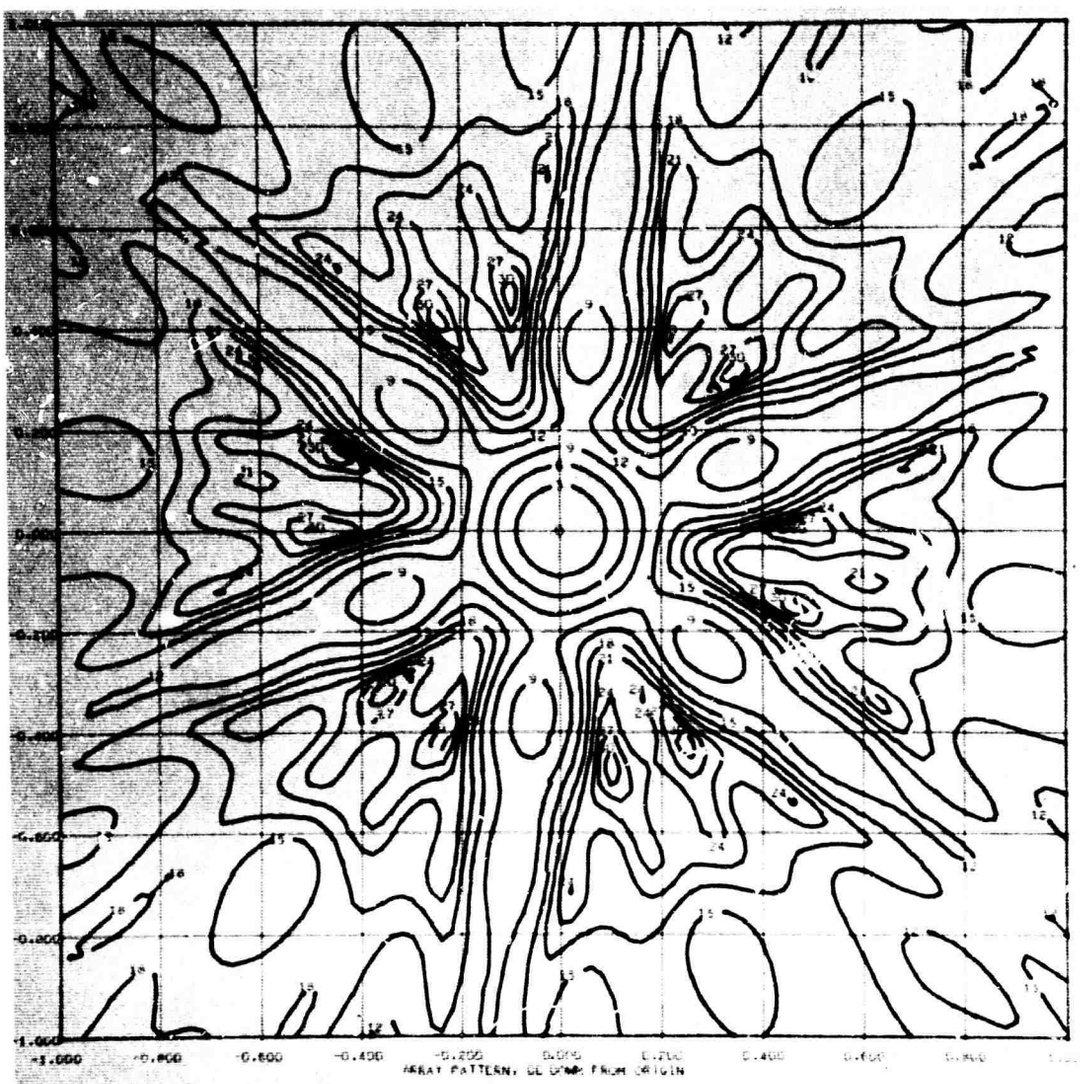

Figure 11 Subarray pattern. $\sigma = 0.1$

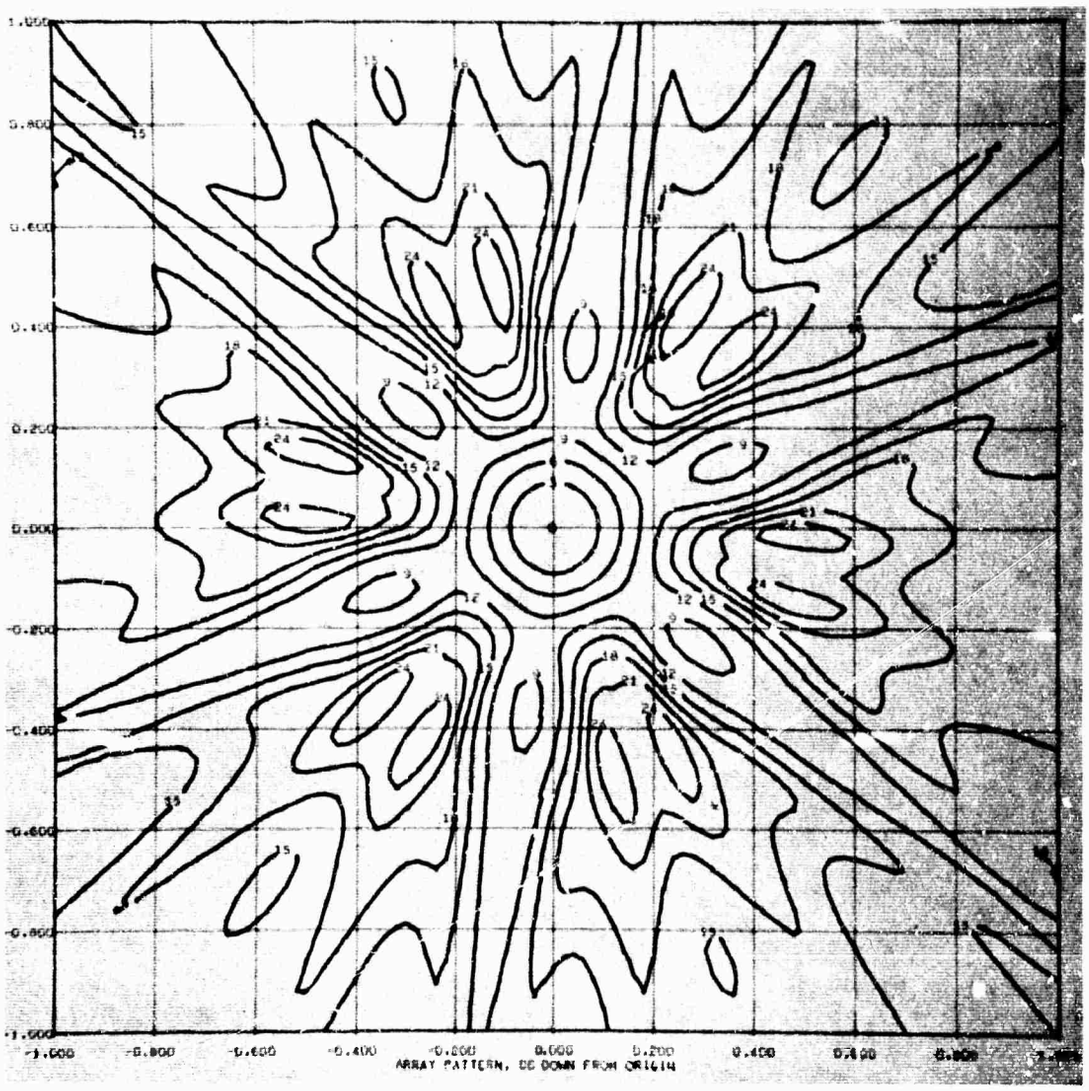

Figure 12 Subarray pattern. $\sigma = 0.2$

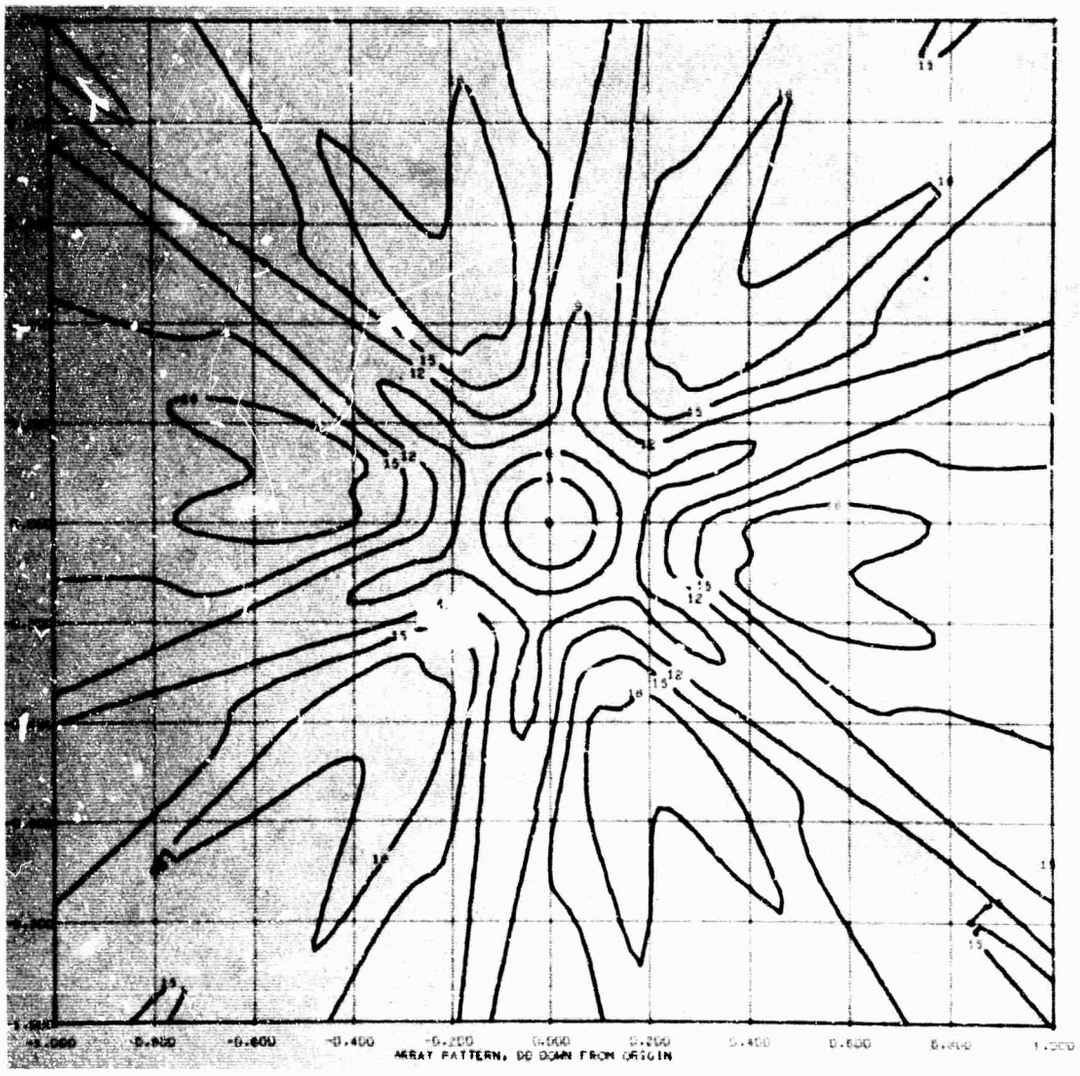

Figure 13 Subarray pattern. $\sigma = 0.3$

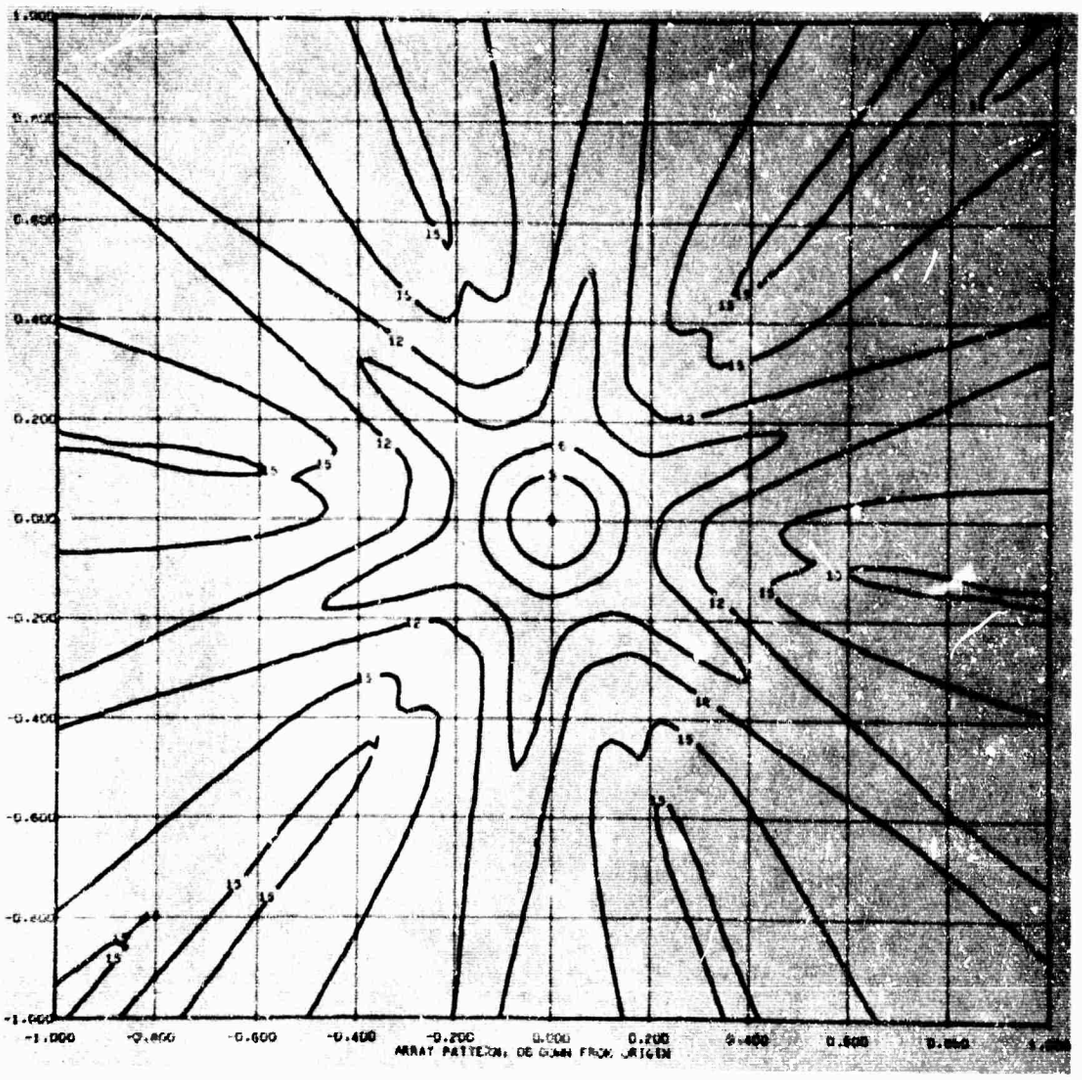

Figure 14 Subarray pattern. $\sigma = 0.4$

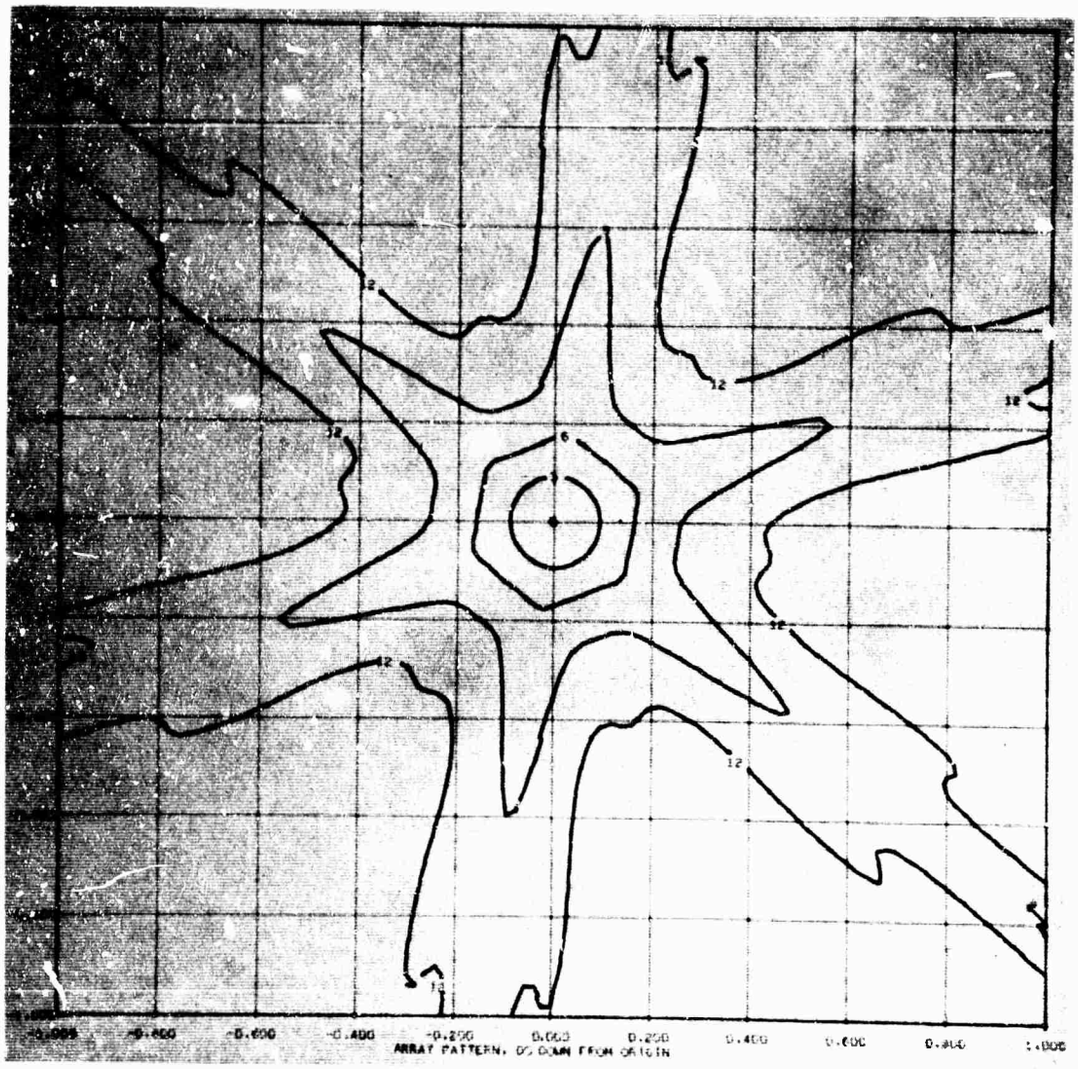

Figure 15 Subarray pattern. $\sigma = 0.5$

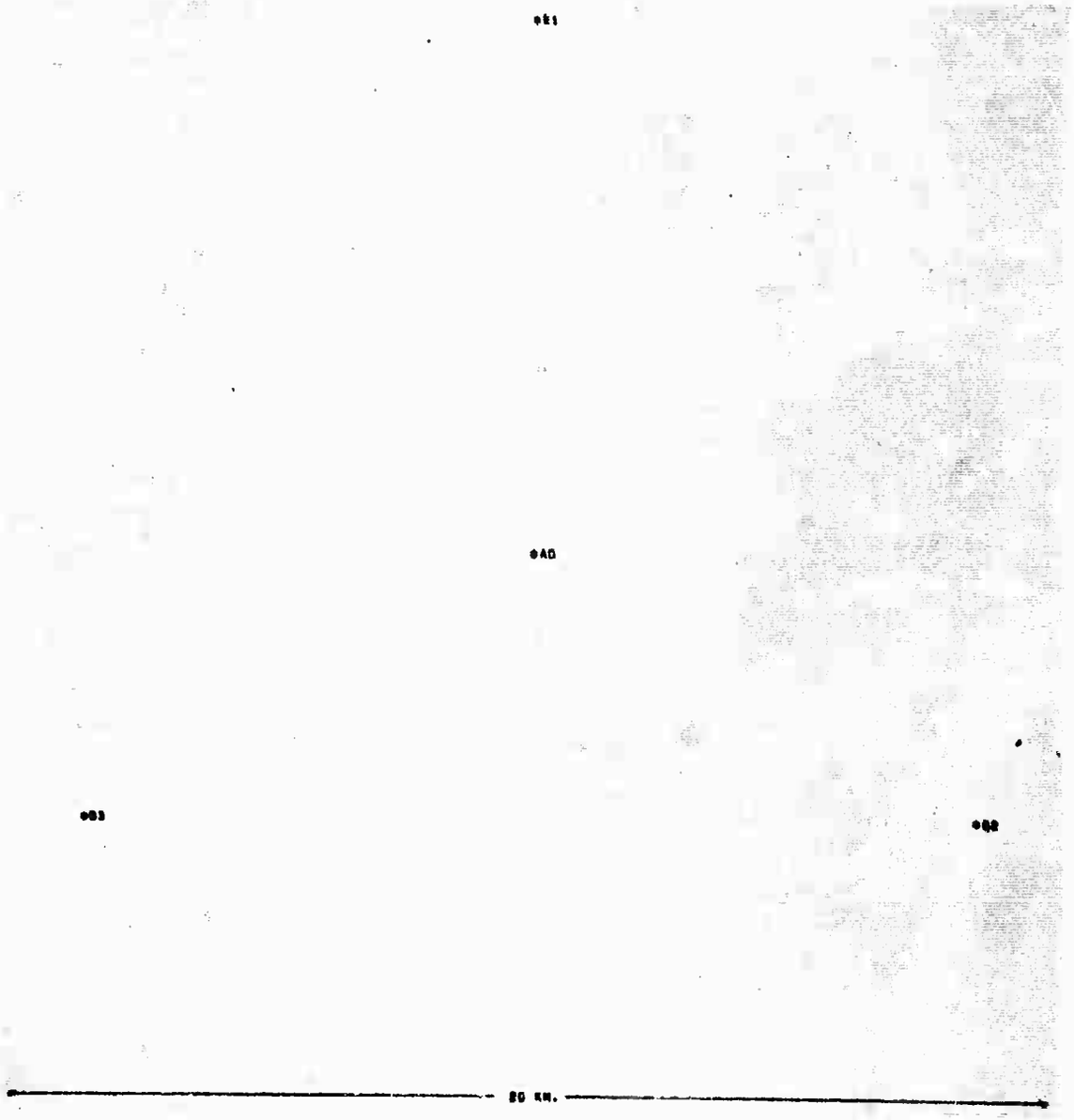

Figure 16 Four-element array.

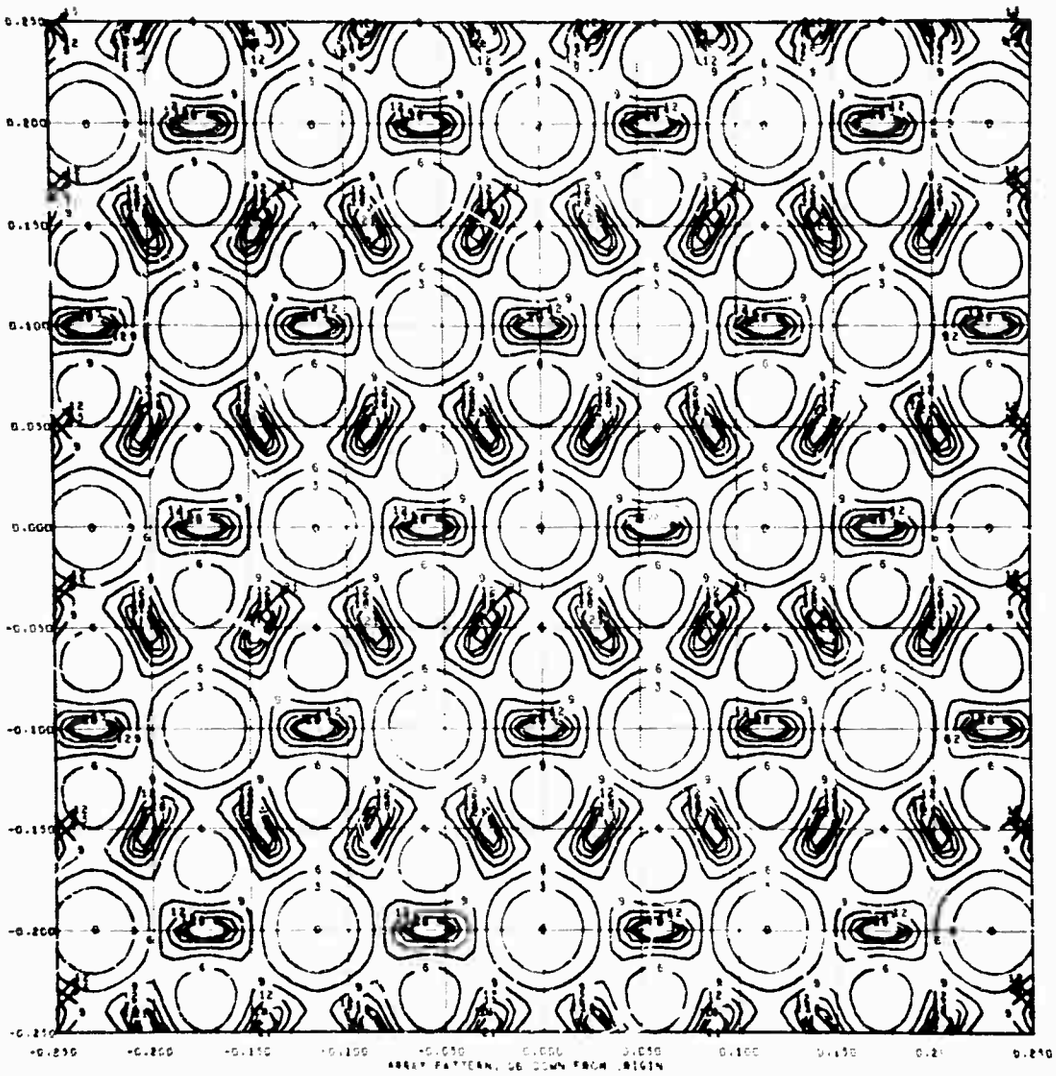

Figure 17 Four-element array pattern. $\sigma = 0.0$

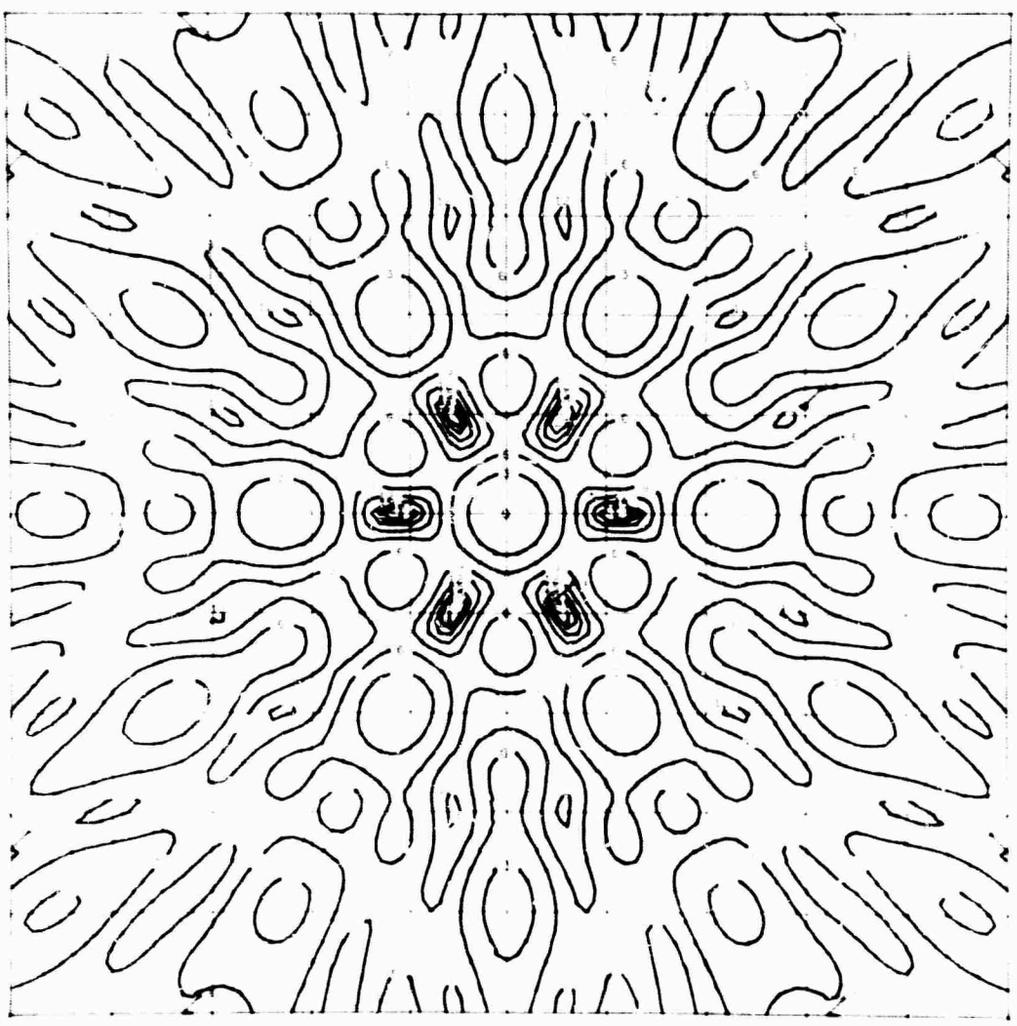

Figure 18 Four-element array pattern. $\sigma = 0.1$

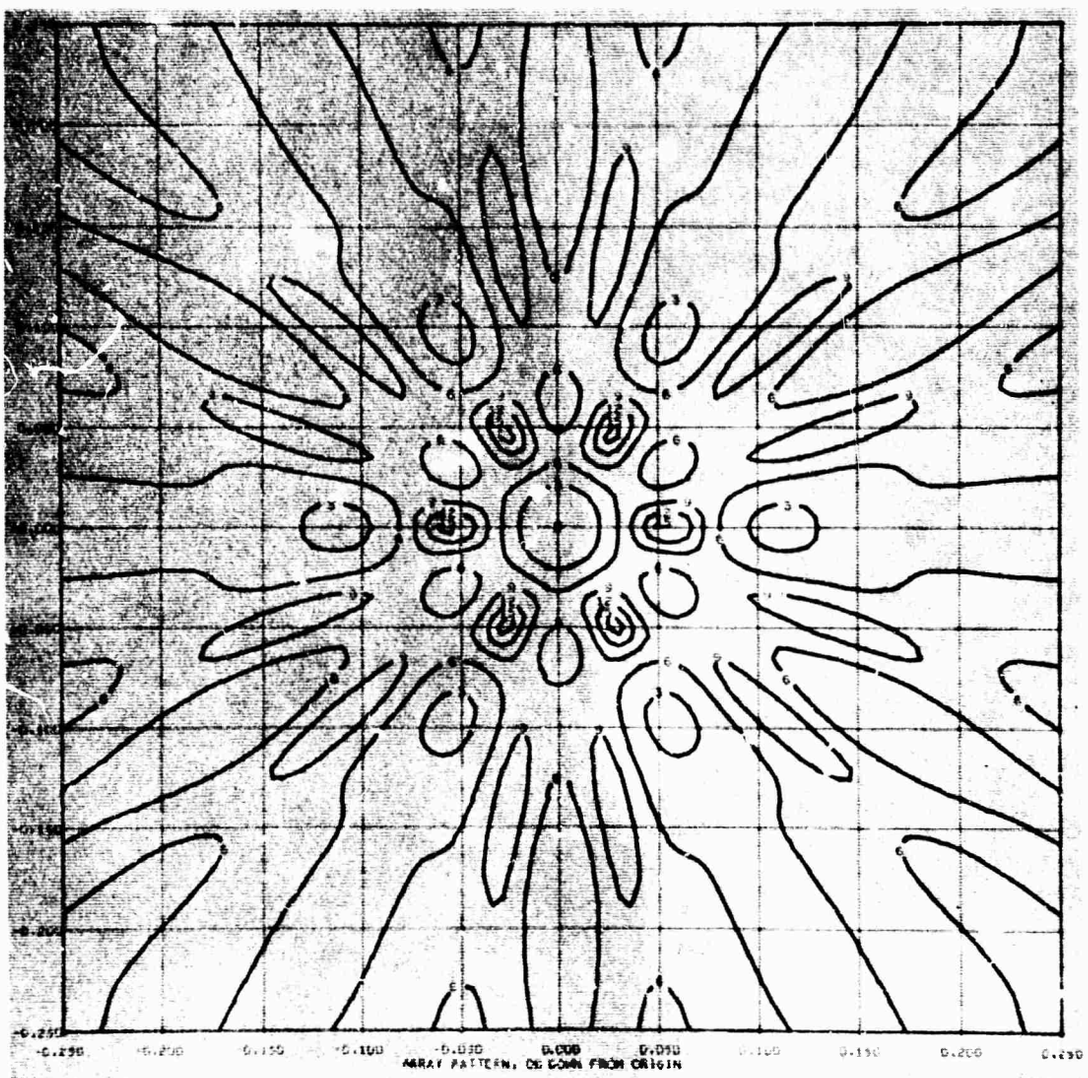

Figure 19 Four-element array pattern. $\sigma = 0.2$

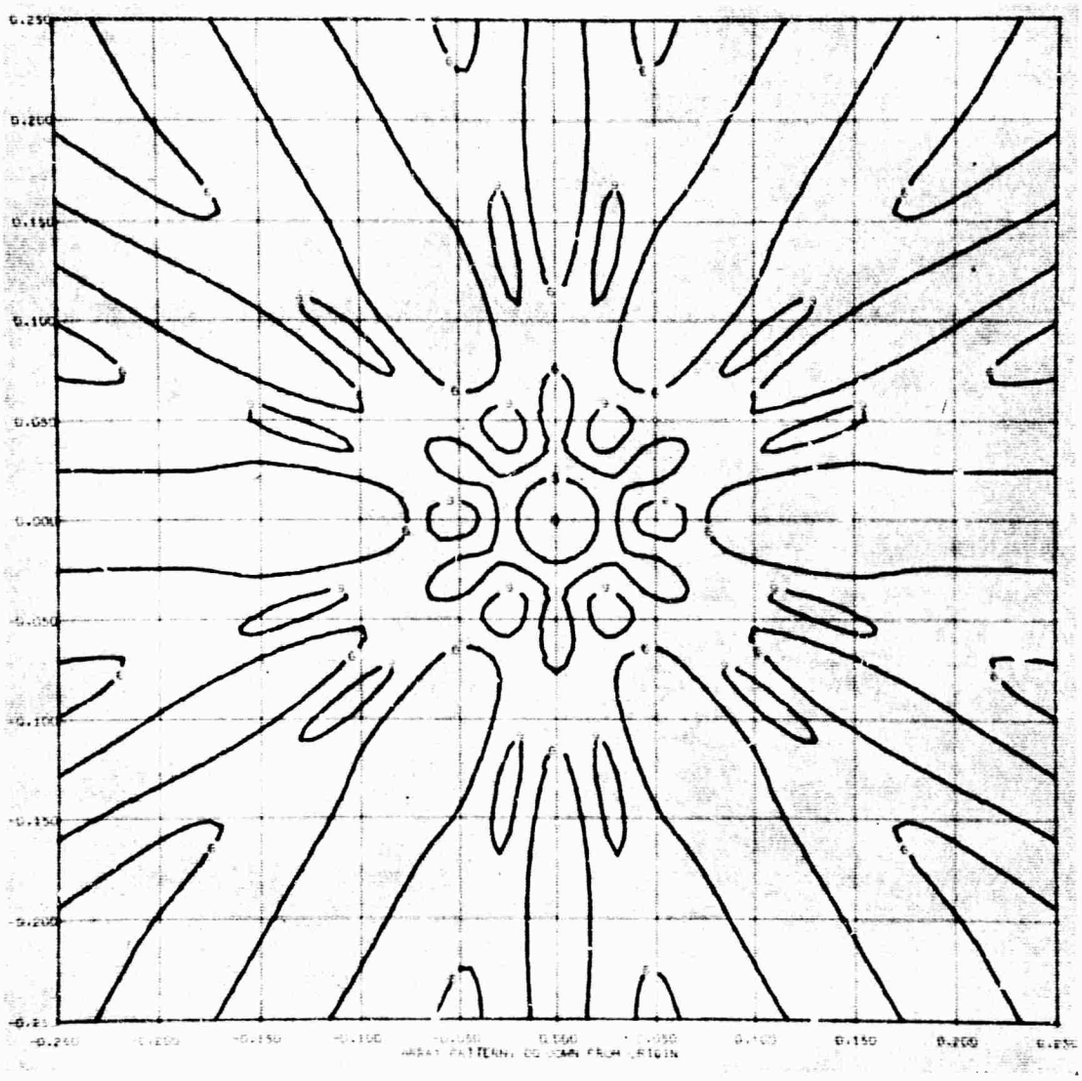

Figure 20 Four-element array pattern. $\sigma = 0.3$

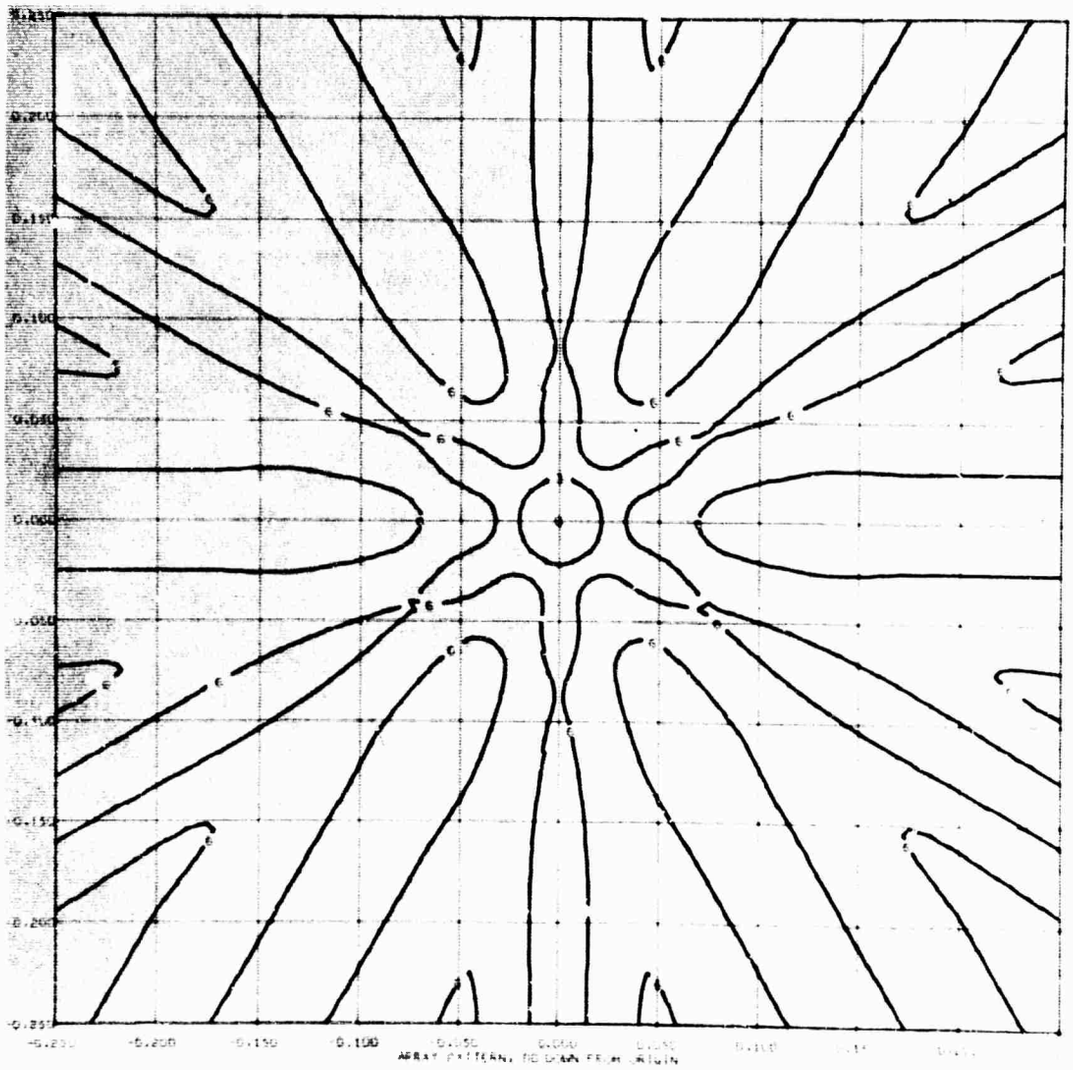

Figure 21 Four-element array pattern. $\sigma = 0.4$

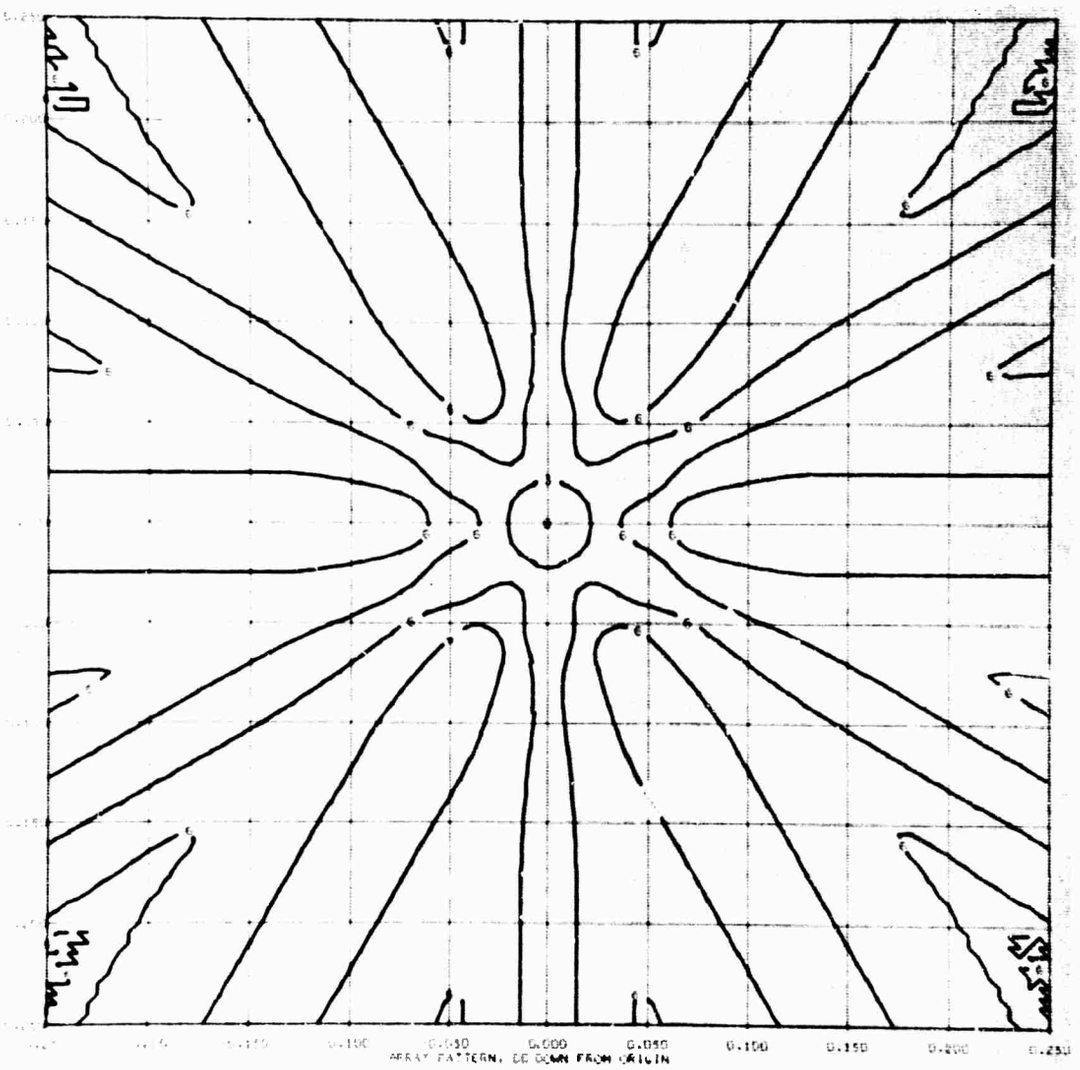

Figure 22 Four-element array pattern. $\sigma = 0.5$

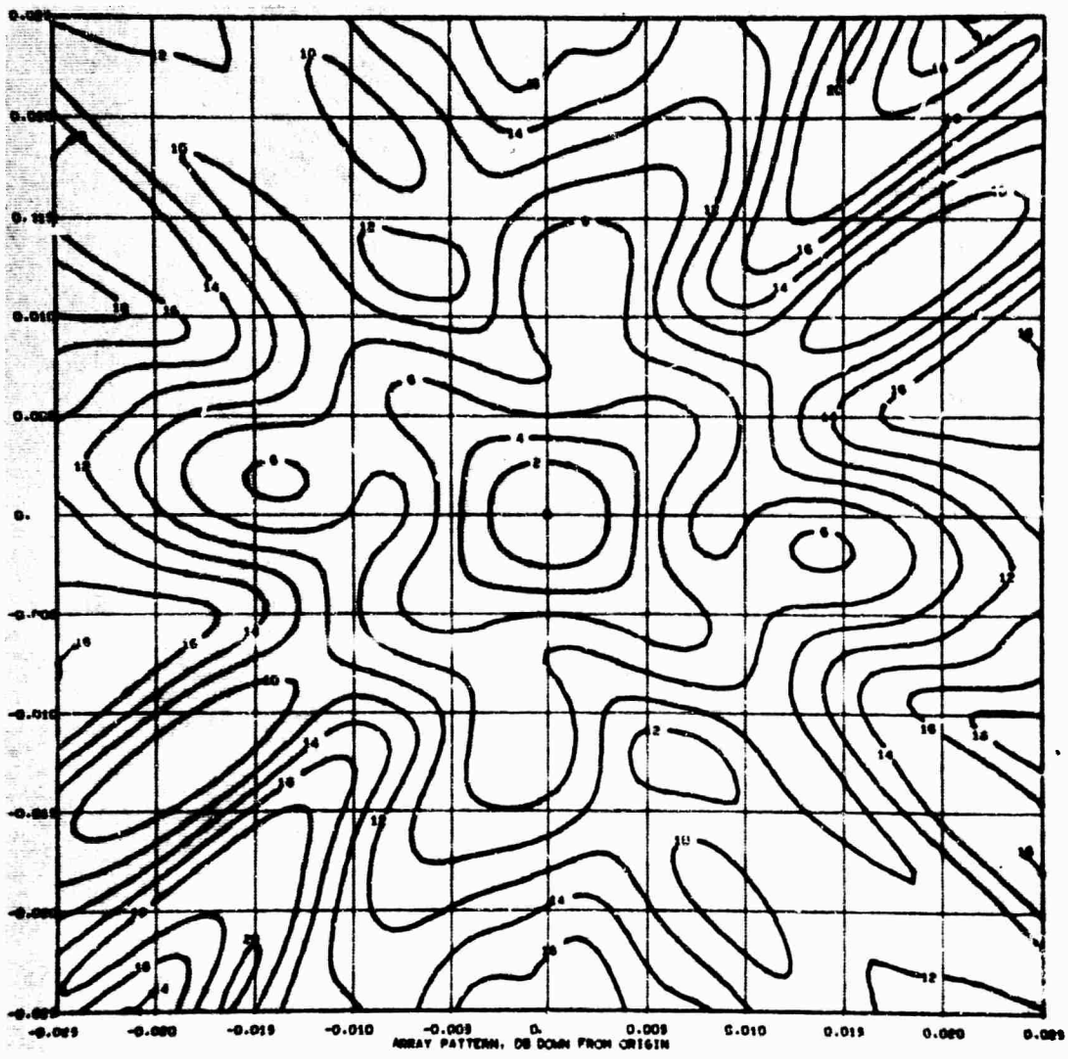

Figure 23 LASA pattern in wavenumber space.

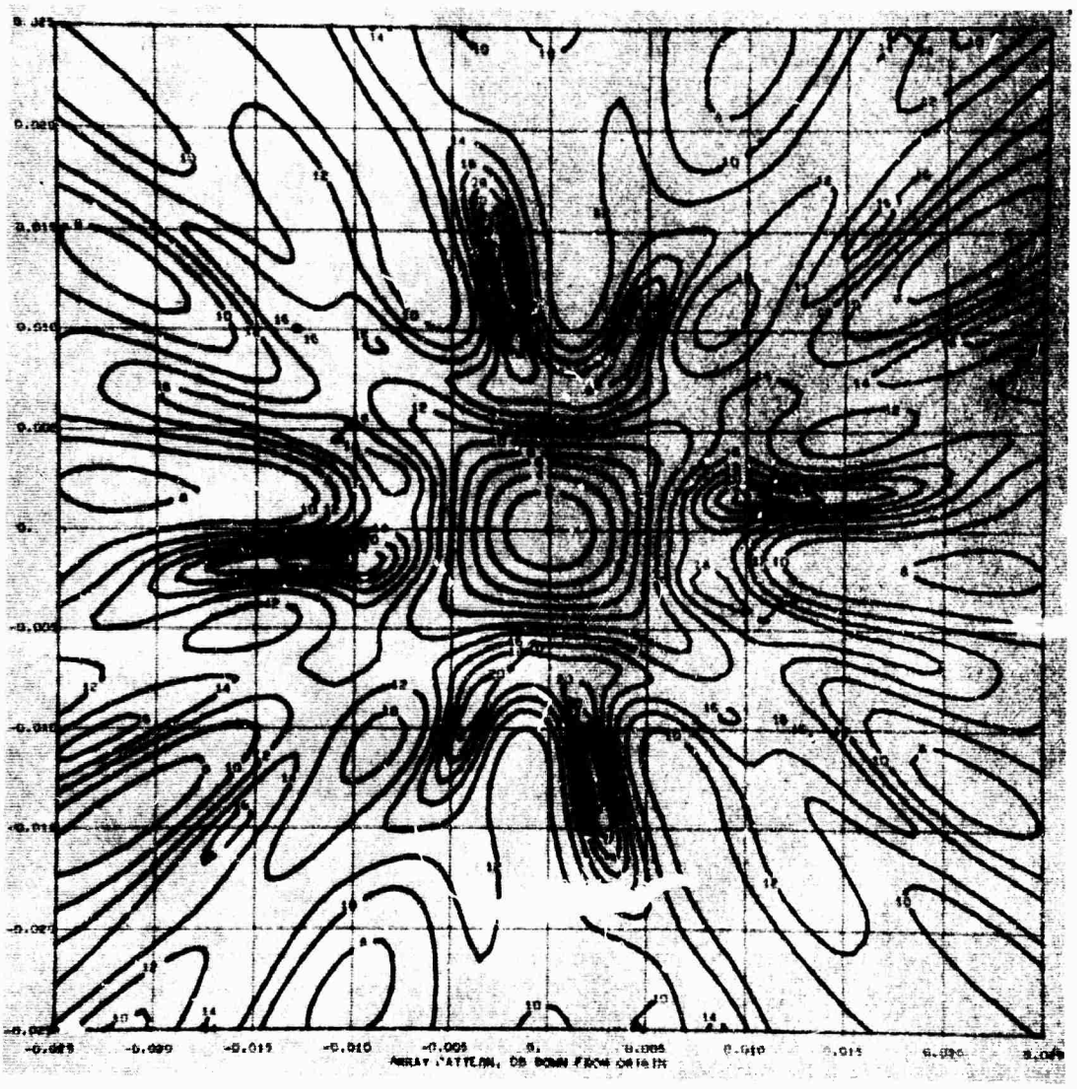

Figure 24 Wavenumber pattern of an array consisting of the LASA D-, E-, and F-sites.

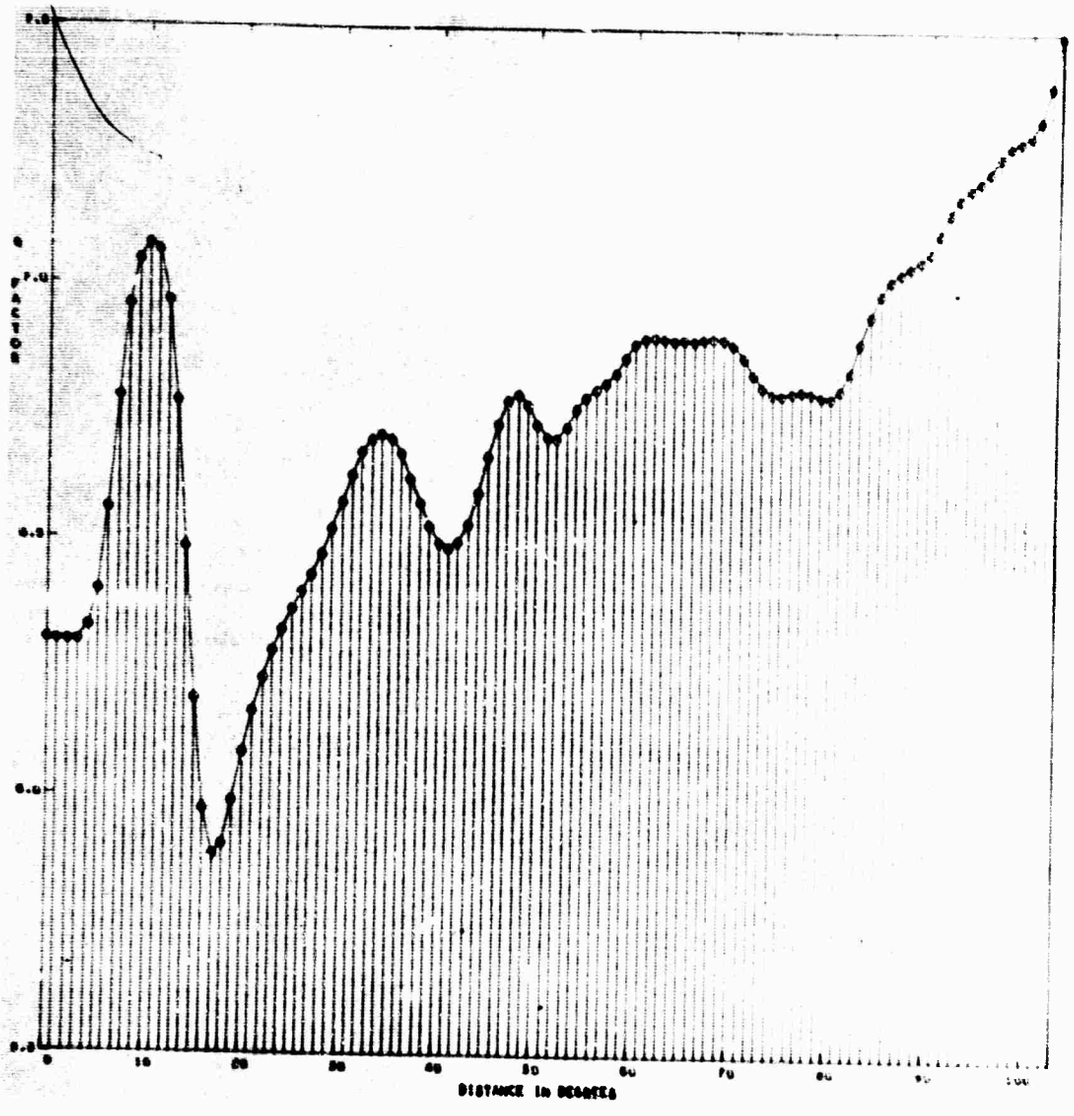

Figure 25 Q-factor, dependence on distance.

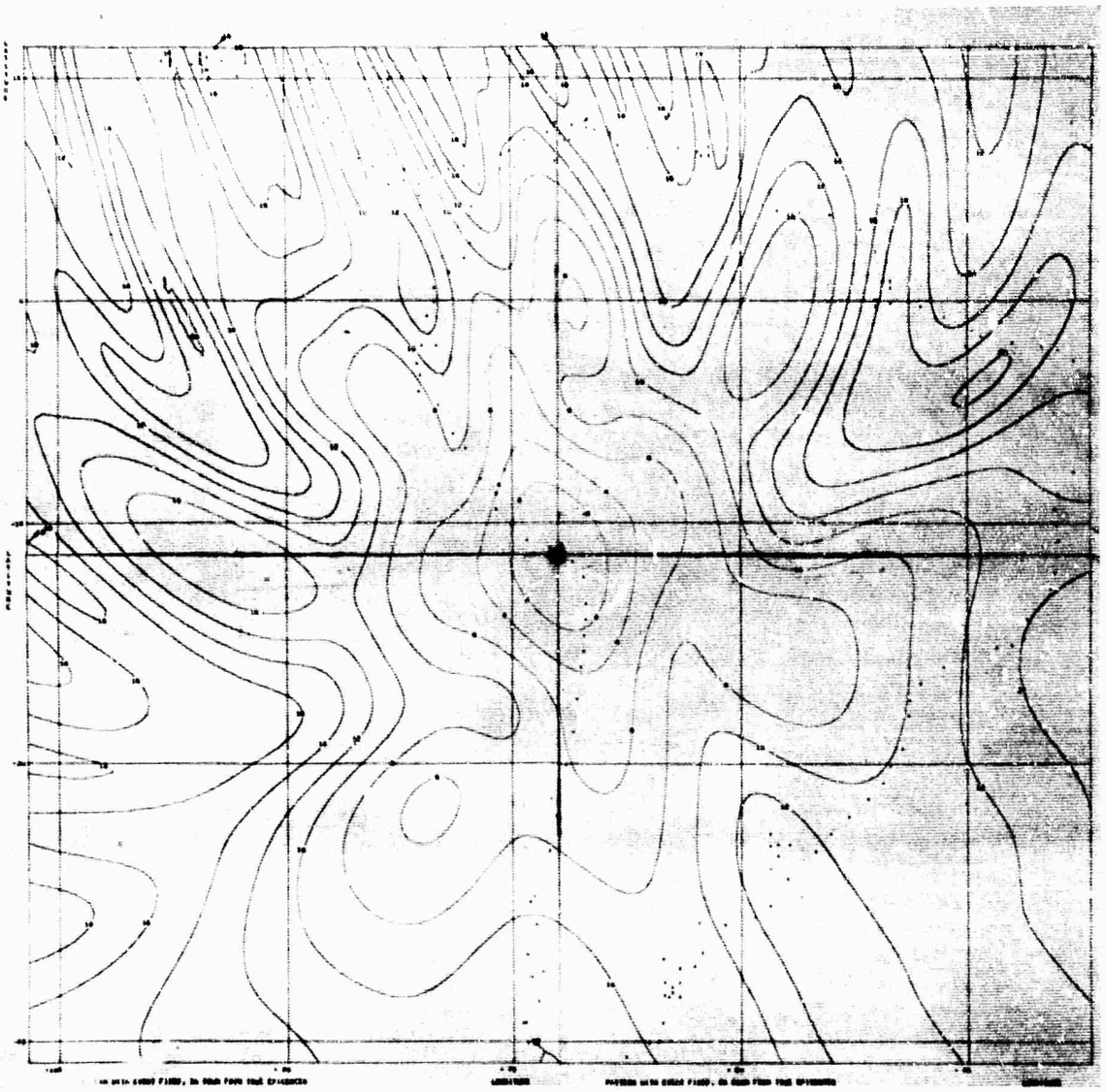

Figure 26 Real space LASA pattern. Epicenter at 70^{o} from array.

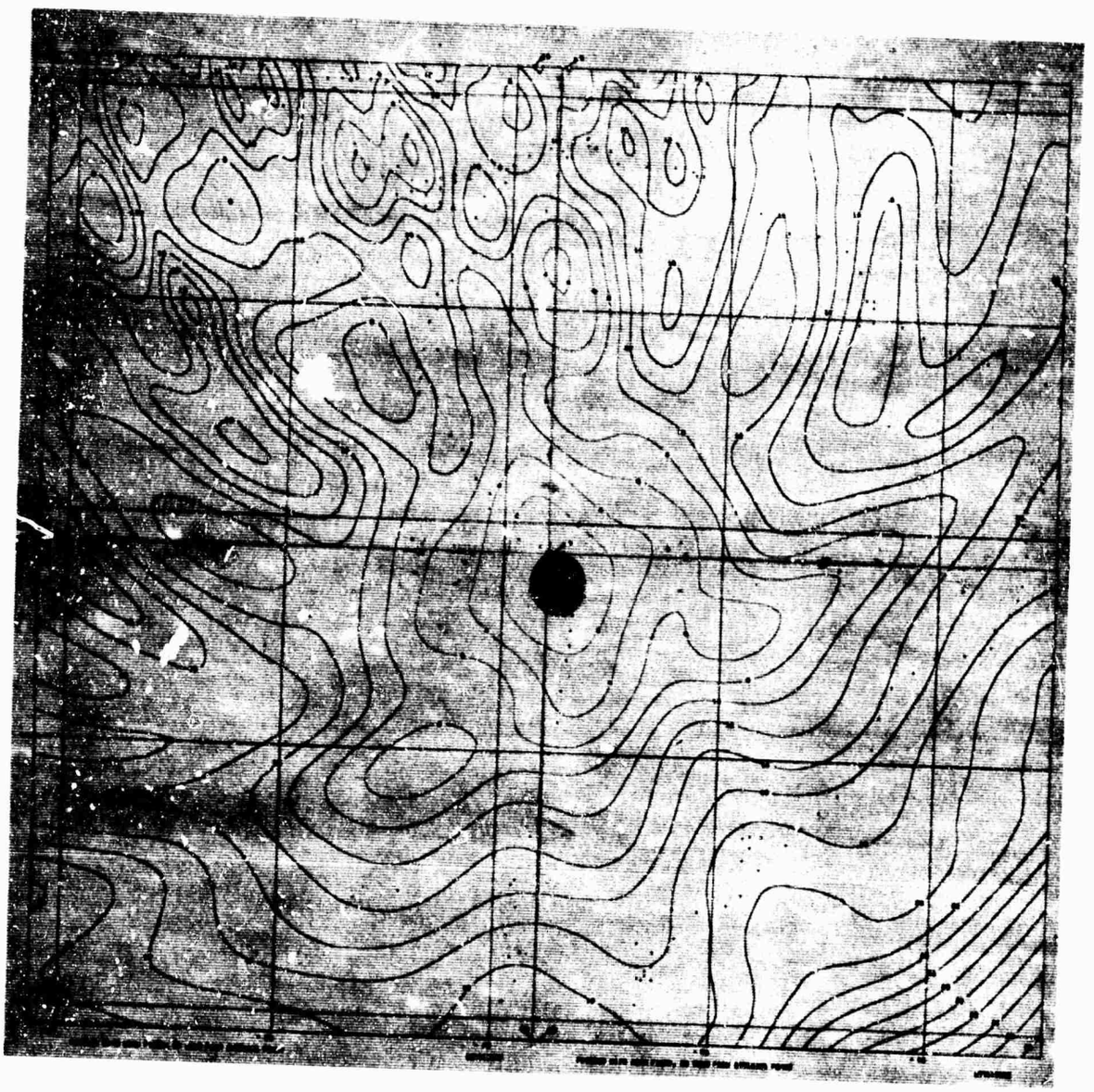

Figure 27 Real space LASA pattern including attenuation. Beam steered at epicenter of Figure 26.

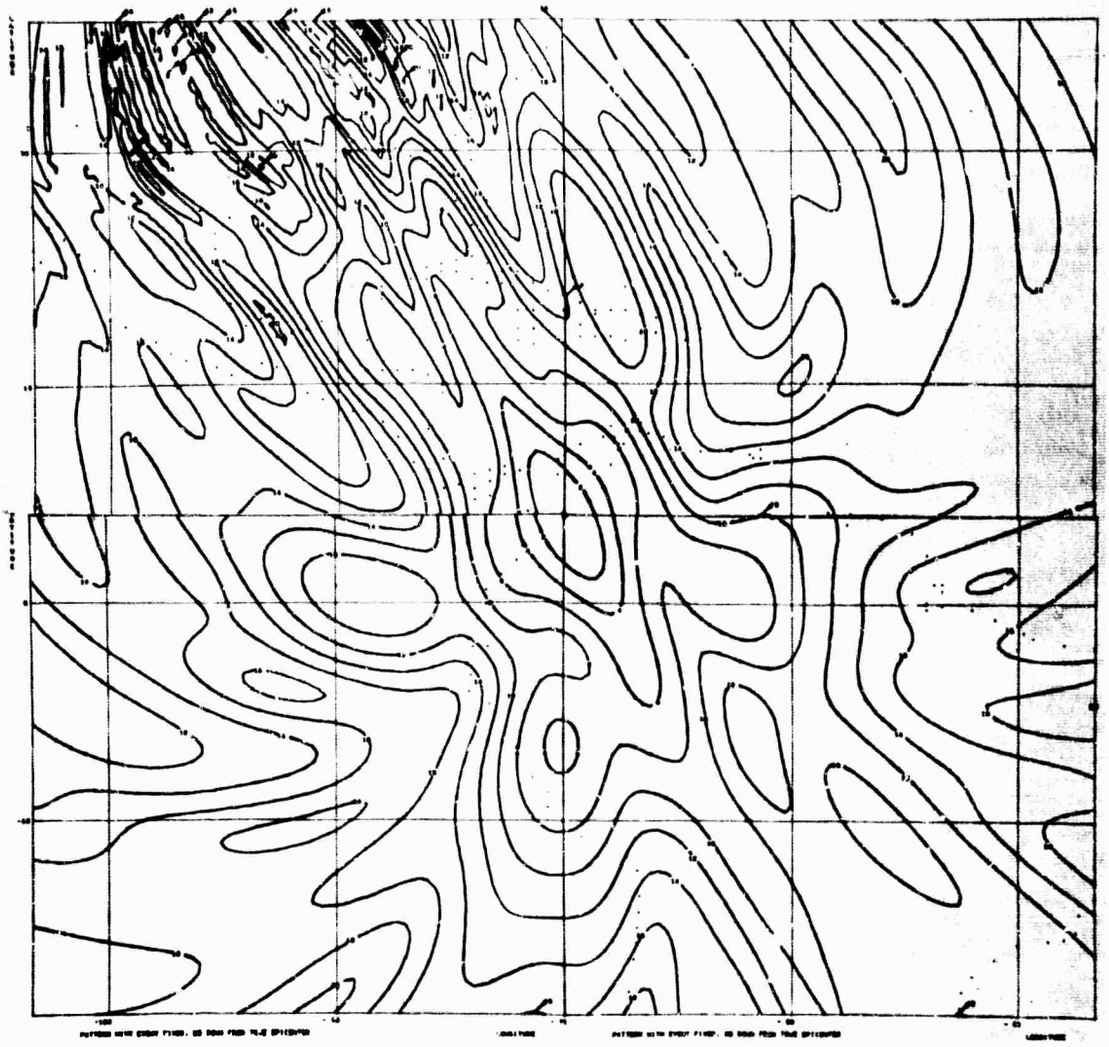

Figure 28 Real space LASA pattern. Epicenter at 48^{o} from array

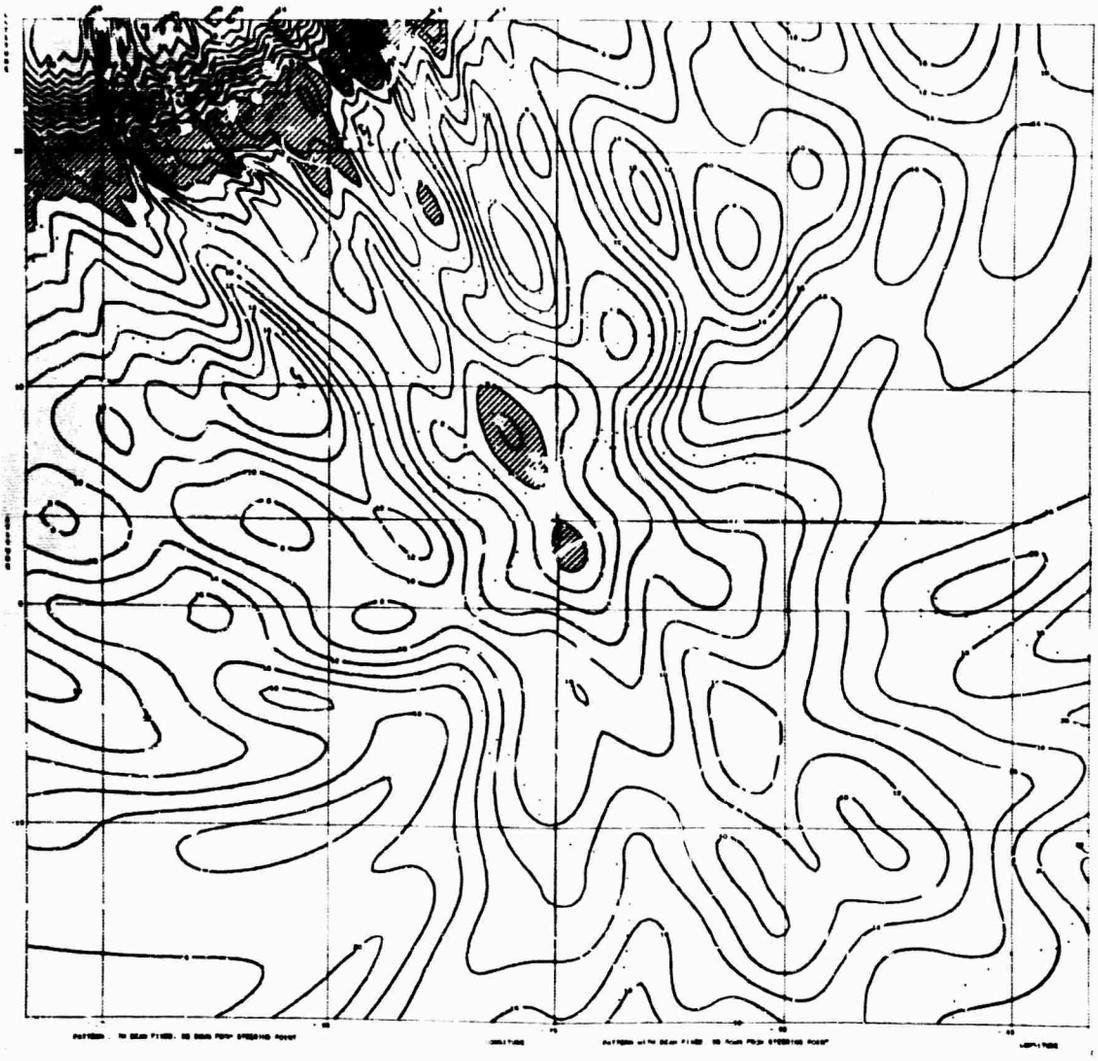

Figure 29 Real space LASA pattern including attenuation. Beam steered at epicenter of Figure 28.

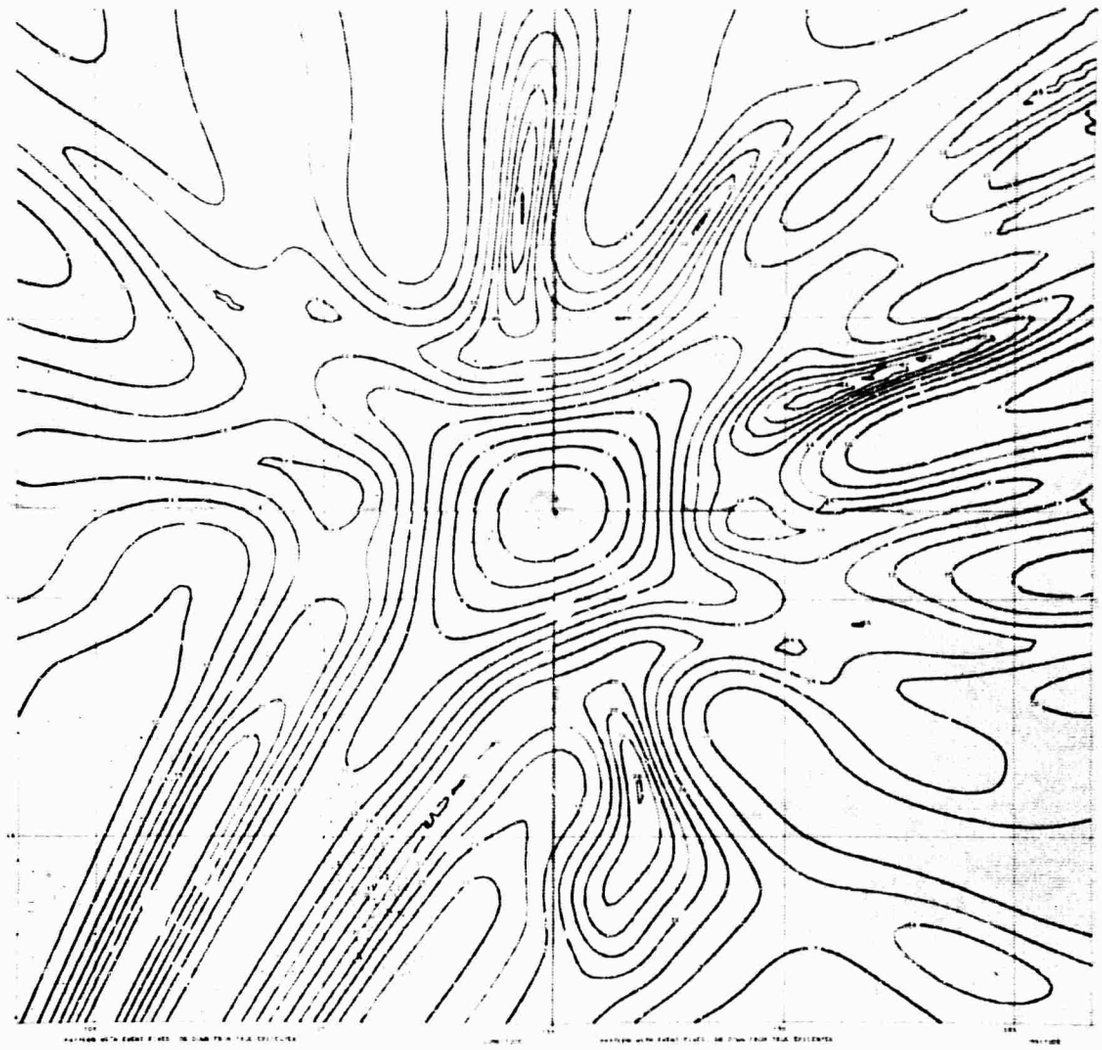

Figure 30 Real space pattern of partial LASA array. Epicenter at 80^{o} from the array.

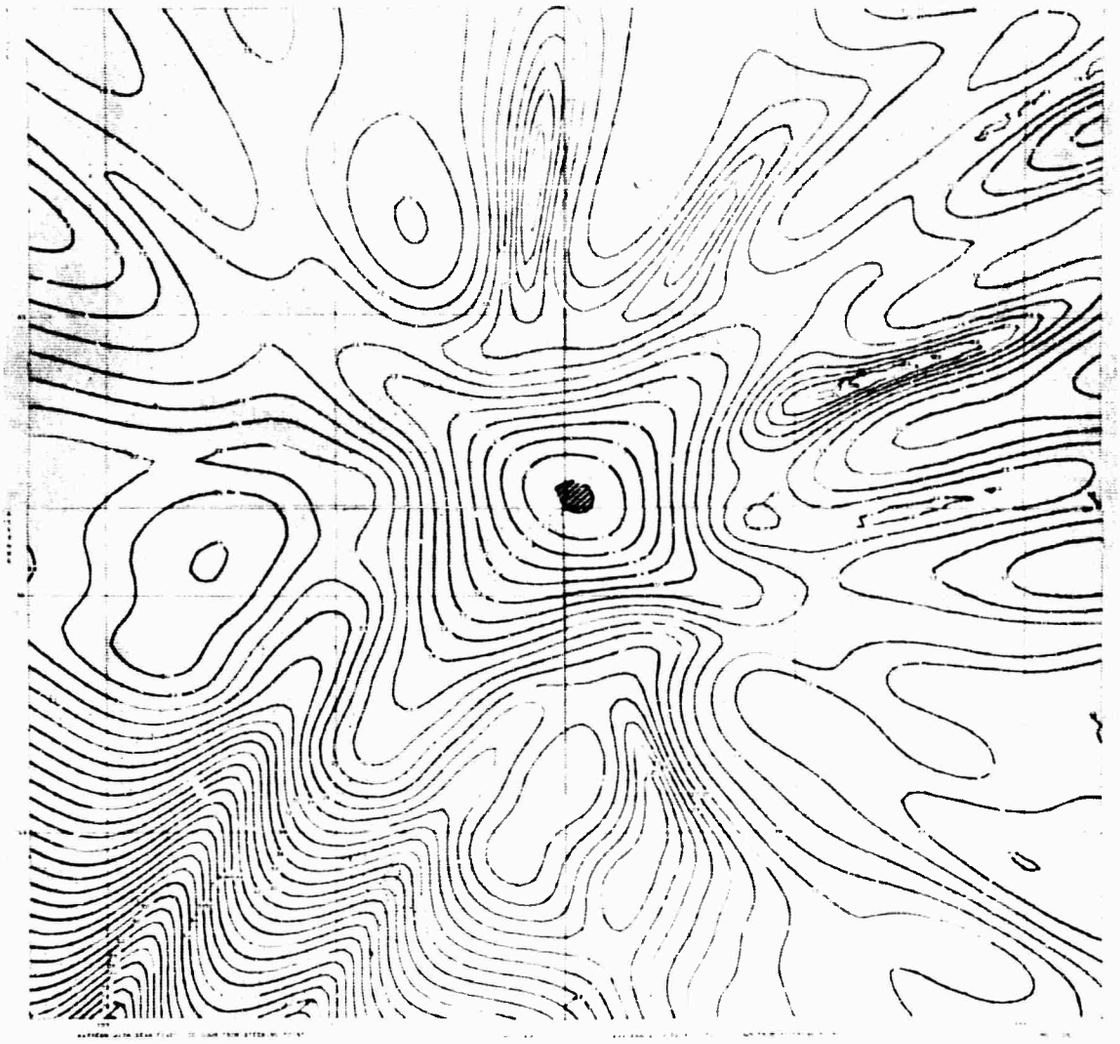

Figure 31 Real space partial LASA pattern, including attenuation. Beam steered at epicenter of Figure 30.

DOCUMENT CONTROL DATA – R&D

(Security classification of title, body of abstract and indexing annotation must be entered when the overall report is classified)

1. ORIGINATING ACTIVITY *(Corporate author)*
Lincoln Laboratory, M.I.T.

2a. REPORT SECURITY CLASSIFICATION
Unclassified

2b. GROUP
None

3. REPORT TITLE
Response of Seismic Arrays to Wide-Band Signals

4. DESCRIPTIVE NOTES *(Type of report and inclusive dates)*
Technical Note

5. AUTHOR(S) *(Last name, first name, initial)*
Kelly, Edward J.

6. REPORT DATE	7a. TOTAL NO. OF PAGES	7b. NO. OF REFS
29 June 1967	52	1

8a. CONTRACT OR GRANT NO.	9a. ORIGINATOR'S REPORT NUMBER(S)
AF 19(628)-5167	Technical Note 1967-30
b. PROJECT NO. ARPA Order 512	9b. OTHER REPORT NO(S) *(Any other numbers that may be assigned this report)*
c.	ESD-TR-67-320
d.	

10. AVAILABILITY/LIMITATION NOTICES
This document has been approved for public release and sale; its distribution is unlimited.

11. SUPPLEMENTARY NOTES	12. SPONSORING MILITARY ACTIVITY
None	Advanced Research Projects Agency, Department of Defense

13. ABSTRACT

Response patterns are computed for the LASA and other arrays and for a class of wide-band signals. Results are displayed as contour plots in wavenumber space and in real space, with and without P-wave attenuation.

14. KEY WORDS

LASA
seismic arrays
beamforming
wide-band signals
Gaussian processes
seismometers
wavenumber